Technical Report

CRWR 240

BEHAVIOR OF CHROMIUM DURING SUPERCRITICAL WATER OXIDATION

by

Sam Rollans
Research Assistant

and

Earnest F. Gloyna
Principal Investigator

July 1993

CENTER FOR RESEARCH IN WATER RESOURCES

Bureau of Engineering Research • The University of Texas at Austin
Balcones Research Center • Austin, TX 78712

ACKNOWLEDGMENTS

This project was funded in part by a joint contract with the United States Environmental Protection Agency and The University of Texas Separations Research Program, an industrial consortium. Also, support was derived from Federal funds through the Gulf Coast Hazardous Substance Research Center, which is supported under cooperative agreement R815197 with the U.S. Environmental Protection Agency.

Additional monies were supplied by research grants from the Tennessee Valley Authority, Eco-Waste Technology, and the Bettie Margaret Smith Chair in Environmental Health Engineering, UT Austin.

ABSTRACT

Studies indicate that the supercritical water oxidation (SCWO) process is an advanced technology capable of totally destroying undesirable organic components and stabilizing inorganic residuals in sludges derived from municipal and industrial wastewater treatment plants. In this process, sludges are subjected to temperatures and pressures greater than 374°C (705.5°F) and 22.1 MPa (3205 psi). Organic substances can be oxidized to inorganic materials or a combination of inorganic and low-molecular-weight organic substances. Under these operating conditions, it may be possible for chromium and other metals in the waste sludges and reactor alloys to be converted to soluble species.

A potential problem may be the presence of soluble trivalent and hexavalent chromium species in the treated effluents. This question is addressed in this report which investigates the partitioning and speciation of chromium in the SCWO environment.

Municipal and industrial wastewater sludges were subjected to a wide range of SCWO conditions. The resulting effluents were separated into liquid and solid fractions, and the concentrations of chromium species were determined.

The SCWO research objectives were to determine the oxidation state of soluble chromium and the behavior of these chromium species. The pH of the effluent determined the oxidation state of the soluble chromium species. At an effluent pH value of < 7, soluble trivalent chromium was the only species generated. Conversely, at an effluent pH value of > 7, soluble trivalent and hexavalent chromium species were generated. Soluble trivalent chromium was removed by co-precipitation with insoluble and associated soluble salts. Similarly, hexavalent chromium was removed by precipitation of chromate salts. Neither adsorption nor desorption of trivalent chromium on surfaces of particulates in the SCWO effluents was detected.

TABLE OF CONTENTS

LIST OF TABLES

LIST OF FIGURES

1.0 INTRODUCTION

Supercritical water oxidation (SCWO), a new and innovative waste treatment technology, is a potential option for the management of wastewater treatment plant sludges. Little information is available, however, on the SCWO environmental conditions and characteristics that determine both the oxidation state and the behavior of soluble chromium species. Without such information, it is difficult to propose the most efficient treatment systems.

SCWO is similar to incineration, but the reactions take place at much lower temperatures (typically 400°C to 600°C) but at higher pressures (typically 25.0 MPa). By utilizing SCWO, the organic materials contained in wastewater sludges are oxidized to relatively innocuous inorganic and low-molecular-weight organic compounds. For all practical purposes, the SCWO reactions occur in a totally contained system. Water serves as the carrier for the influent sludge and effluent ash.

Supercritical water exhibits unique physical properties, including the fact that organic compounds and oxygen become completely miscible. The resulting medium is single-phase with rapid, gas-like transport properties and liquid-like, high collision rates. Under these conditions, oxidation of many organic compounds, particularly the higher molecular weight compounds, occurs rapidly. The viscosity, density, and dielectric constant of water decrease rapidly if its temperature is increased to above 374°C at 25.0 MPa. At these conditions, inorganic salts have low solubilities and suspended solids have high separation efficiencies. These characteristics allow for the efficient removal of such materials from SCWO effluents.

The SCWO treatment conditions that oxidize organic materials in wastewater sludges are also capable of converting heavy metals, particularly chromium, to water-soluble species. Chromium is present in wastewater sludges and high-grade alloys. Municipal and industrial wastewater sludges contain a wide range of chromium concentrations. As an example, the chromium concentrations in dry municipal wastewater sludges in the U.S. range from 10 mg/kg to 99,000 mg/kg (Metcalf and Eddy, 1991). Chromium concentrations of high-grade alloys, proposed for use in SCWO reactors, can range from 15% to 20%.

Chromium can be present as four species in typical SCWO effluents. These species are (a) trivalent chromium salts having a wide range of solubilities, (b) nonsoluble trivalent chromium salts, (c) adsorbed trivalent chromium, and (d) hexavalent chromium salts having a wide range of solubilities. The total concentration and distribution of these chromium species in the effluent will be determined by SCWO treatment conditions and characteristics of the influent wastewater sludges.

Presence of these chromium species can impact the quality of effluents. The potential impacts must be considered prior to discharge of SCWO effluents to surface waters, publicly owned treatment works (POTW) systems, or other treatment processes. The particular chromium species generated at various SCWO conditions and the behavior of these species may be of considerable design importance. The quality of the effluent liquid and settleable ash may be adversely impacted by some chromium species. Conversely, some chromium species can be handled easily. Notably, insoluble trivalent chromium salts and absorbed trivalent chromium can be removed efficiently from SCWO effluents by solids separation technologies. Little information is available, however, on the behavior of soluble trivalent and hexavalent species in supercritical waters. These chromium species are EPA-listed priority pollutants and their concentrations in SCWO effluents are limited by water quality considerations.

Hexavalent chromium is of particular concern. It is much more toxic to aquatic flora and fauna than trivalent chromium. Therefore, it is important to determine the chromium speciation. Similarly, it is necessary to understand the behavior of these chromium species in the SCWO environment.

1.1 Objectives

The purpose of this research was to study the behavior of chromium species during the SCWO of wastewater sludges. Specifically, the objectives were to determine:

- chromium species generated at various SCWO treatment conditions and effluent characteristics and
- the behavior of chromium species in supercritical water.

1.2 Scope

This research used a pilot-scale, continuous-flow reactor. Two types of wastewater sludges were used: (a) an anaerobically digested municipal sludge and (b) an excess, activated industrial sludge. The test variables were limited to maximum reactor temperature and sludge feed rate. Maximum reactor temperature varied from 300°C to 450°C, sludge feed rate ranged from 60 gm/min to 120 gm/min. The oxygen feed was set at a minimum of 200% of the stoichiometric demand for all waste feeds. Pressure was maintained at 25.0 MPa (3600 ±100 psi) for all tests. The influent and effluent streams were characterized for chemical oxygen demand (COD), total suspended solids (TSS) or volatile solids (VS), ammonia, chromium species, and selected anions and cations.

1.3 Rationale

The costs of managing industrial and municipal wastewater sludges are increasing due to more stringent regulatory requirements. Future wastewater sludge management options must have as goals minimal environmental impacts and economic viability. For SCWO to achieve these goals, it must be demonstrated that soluble chromium species can be removed from SCWO effluents to required levels in a safe, efficient, and cost-effective manner.

2.0 LITERATURE ANALYSIS

This chapter discusses the properties of supercritical water and its application for the treatment of organic waste. The behavior of chromium in aqueous systems is summarized. Factors affecting chromium corrosion rates in SCWO environments are analyzed. The literature related to chromium corrosion and behavior of chromium corrosion products in wet air oxidation (WAO), sub-critical (sub-CWO), and SCWO environments is reviewed.

2.1 Properties Of Supercritical Water

The critical point of water, as shown in Figure 2.1, is 374.2°C (705.5°F) and 221 bar (22.1 MPa or 3209 psi). At temperatures and pressures greater than those of the critical point, water exhibits properties of a supercritical fluid. Water at supercritical conditions is a fluid that is neither a liquid nor gas. In the supercritical region, the boundary between the liquid and phases is absent. The density, dielectric constant, and ionic product of water are altered in the supercritical region. The diffusion coefficients, solubilities, and dissociation constants for organic and inorganic substances are altered significantly in supercritical water.

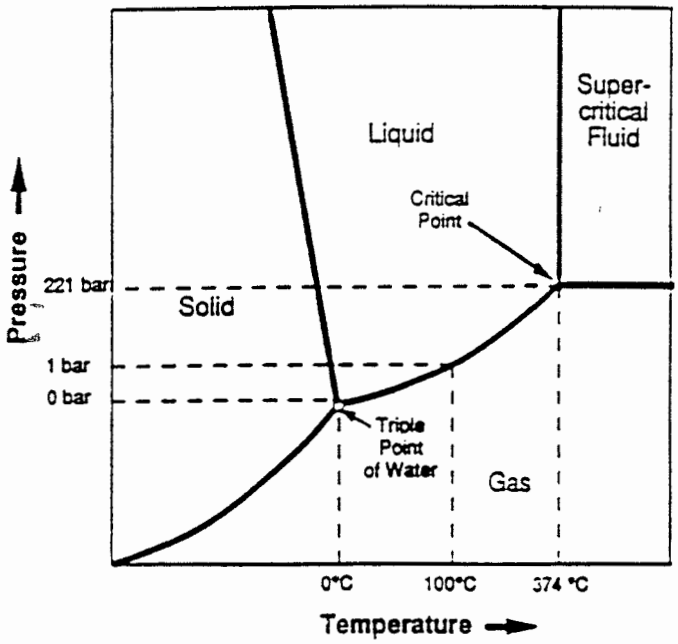

Figure 2.1 Phase Diagram of Water
(Josephson, 1982)

A temperature-density diagram of water is shown in Figure 2.2. In the temperature range of 300°C to 450°C at 25.0 MPa, the density of water decreases from about 0.8 gm/cm^3 to 0.1 gm/cm^3. The most rapid decrease in density occurs from 374°C to 400°C. At 374°C and 250 atm, water density is about 0.5 gm/cm^3, whereas at the critical point it is 0.32 gm/cm^3 (Franck, 1963).

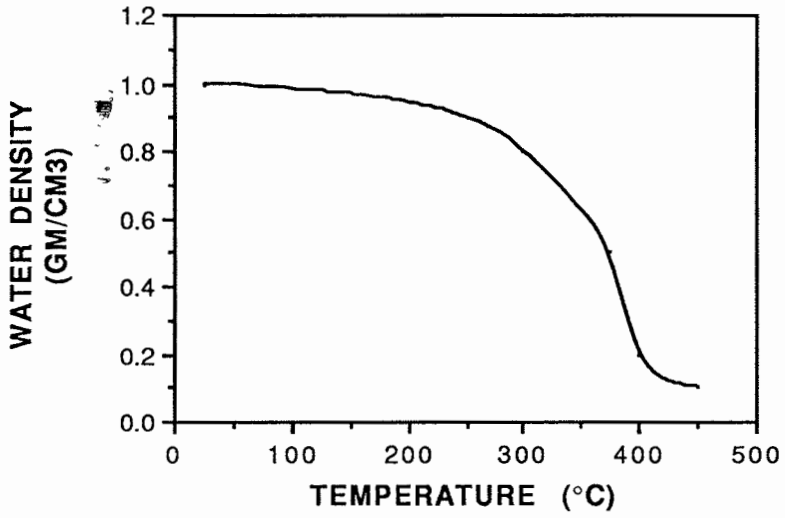

Figure 2.2 Water Density at 25.0 MPa
(Thomason and Modell, 1984)

Supercritical water properties have been elucidated by measuring the dielectric constant. The dielectric constant (ε) is a measure of the degree of molecular association. Water at ambient conditions has a dielectric constant of about 80 (Uematsu and Franck, 1980). This high dielectric constant is largely the result of strong hydrogen bonding between water molecules. The dielectric constant of water decreases rapidly as temperature increases. The density of water, however, decreases slowly as the temperature increases. Hydrogen bonding forces are strong only when water molecules are close to each other. At the critical point, the dielectric constant of water is 5. Raman spectra of water at critical conditions indicate little, if any, residual hydrogen bonding (Franck, 1976). Molecular association, due to dipole-dipole interactions, is the major contributor to the dielectric constant of water at critical conditions. Dipole-dipole interactions gradually decrease as the density of water decreases.

A temperature-dielectric constant diagram of water is shown in Figure 2.3. In the temperature range of 25°C to 490°C at 25.0 MPa, the dielectric constant of water decreases from about 80 to 2. The most rapid decrease occurs from 25°C to 300°C; at 300°C, the dielectric constant is about 15.

The solvent power of water for organic chemicals is consistent with variations in the dielectric constants of water and organic chemicals. Benzene (ε = 2.28) solubility is a good example. Figure 2.4 illustrates the solubility of benzene in water at 25.0 MPa. An increase in solubility from 35% at 295°C to complete miscibility at 300°C is apparent.

Other organic chemicals exhibit similar behavior. Aliphatic hydrocarbons, which are less soluble in water than aromatic hydrocarbons at comparable temperatures, require higher temperatures to reach miscibility. Pentane (ε = 1.84) and heptane (ε = 2.04) are completely miscible in water at 350°C and 25.0 MPa.

The diffusion coefficients of inorganic ions and organic molecules are the relative potentials of these materials to move from volumes of high concentrations in water to volumes of low concentrations in water (Weast, 1985). At ambient conditions, the diffusion coefficients are high for inorganic ions, but are low for organic molecules. At supercritical conditions, the reverse is true: inorganic ions have low diffusion coefficients and organic molecules have high diffusion coefficients.

Many gases, which have low solubilities in water at ambient conditions, have total miscibility in supercritical water. Oxygen, nitrogen, helium, hydrogen (Pray et al., 1952), carbon dioxide (Todheide and Franck, 1963), and ammonia (Thomason and Modell, 1984) are completely miscible with water at 374°C and 25.0 MPa.

Supercritical water is an excellent solvent for organic substances; it is, however, a very poor solvent for inorganic salts. The solubility of inorganic salts drops very rapidly as the temperature is increased above 350°C at 25.0 MPa. Decreases in solubility of up to three orders of magnitude are observed in the temperature range of 375°C to 400°C. At 400°C and 25.0 MPa, the solubilities of NaCl, $CaCl_2$, and $CaSO_4$ are approximately 600 ppm, 10 ppm, and 0.033 ppm, respectively.

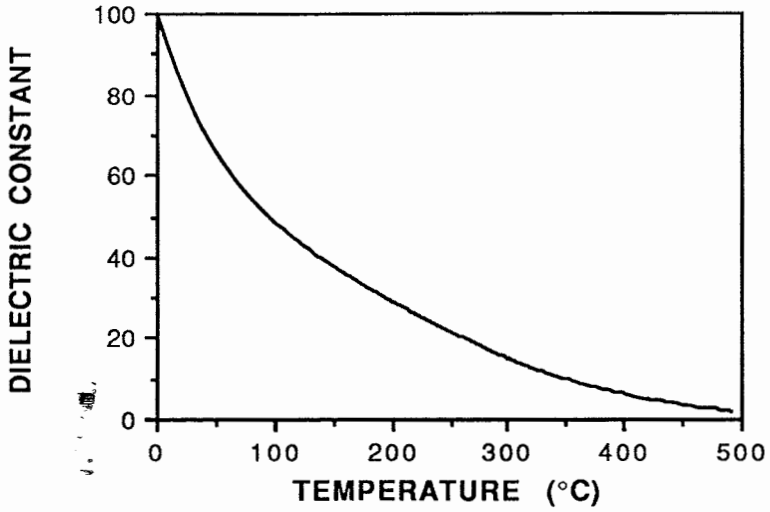

Figure 2.3 Dielectric Constant of Water at 25.0 MPa
(Thomason and Modell, 1984)

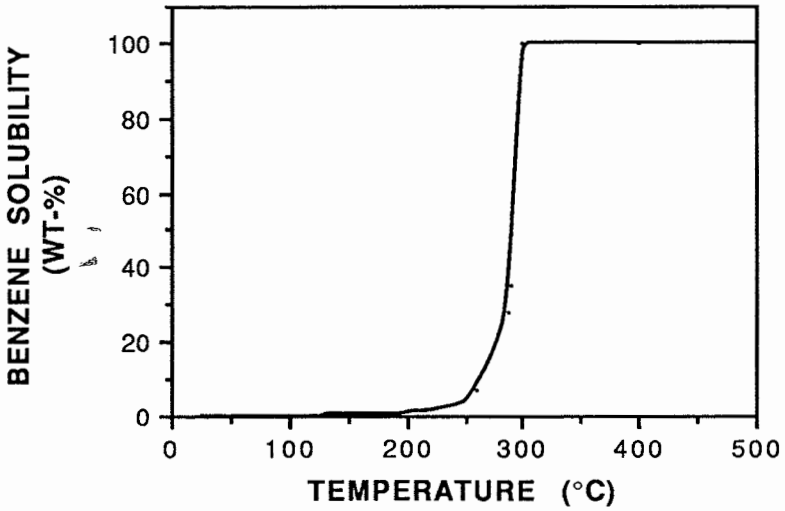

Figure 2.4 Benzene Solubility in Water at 25.0 MPa
(Connolly,1966)

The solvation characteristics of supercritical water change significantly with pressure increases. A pressure increase to 30.0 MPa from 25.0 MPa raises the solubilities of inorganic salts by approximately an order of magnitude. At pressures sufficient to maintain the density of supercritical water at near or above 1.0 gm/cm^3, the solubilities of inorganic salts increase (Marshall, 1975).

Concurrent with decreases in solvating power for inorganic salts, the ability of supercritical water to dissociate inorganic salts decreases as the temperature increases. The dissociation constant of NaCl at a water density of 0.30 gm/cm^3 ranges from less than 10^{-4} at 400° C to less than 10^{-5} at 800°C (Marshall, 1976). Strong electrolytes thus become extremely weak electrolytes in supercritical water.

Supercritical and near-critical water are also poor solvents for bases and acids. At 400°C and 25.0 MPa, the solubility of $Mg(OH)_2$ is approximately 7.0 ppb (Martynova, 1976). At above 400°C, the solubility of $Mg(OH)_2$ remains virtually constant. Marshall (1976) reported that the solubility of $Ca(OH)_2$ in a 0.025 ionic strength $NaNO_3$ solution decreases as the temperature increases. At 350°C (the maximum temperature tested) and 25.0 MPa, the solubility of $Ca(OH)_2$ is ≈150 ppm.

Marshall (1976) reported that HSO_4^- is greatly associated at high temperatures and moderate pressures. The dissociation constant of HSO_4^- at equal ionic strengths of $NaNO_3$ decreases as the temperature is increased. At 350°C (the maximum temperature tested) and 22.1 MPa, the dissociation constant of HSO_4^- was 3.0×10^{-7}.

Supercritical water viscosity is dependent upon its density. The viscosity of water increases as the density increases. At 500°C and at densities of 0.2 gm/cm^3 and 0.8 gm/cm^3, the viscosity of water is about 0.04 cP and 0.10 cP, respectively (Franck, 1973; Todheide, 1972). In low viscosity supercritical water, diffusivities of organic substances and ion mobilities for dissociated inorganic salts will be higher than in high viscosity supercritical water.

Electrical conductance is a measure of the dissociation of inorganic salts in an aqueous environment. The electrical conductance for an inorganic salt solution at supercritical conditions is a function of temperature and density. For a 0.100 M NaCl solution at temperatures ranging from 400°C to 800°C, the highest electrical conductance occurs at densities from 0.7 gm/cm^3 to 0.8

gm/cm^3 (Marshall, 1976). The electrical conductance decreases as densities are lowered to less than 0.7 gm/cm^3 or raised to greater than 0.8 gm/cm^3.

Two different mechanisms occurring at different density ranges are responsible for conductivity decreases (Marshall 1968). Decreases in supercritical water conductivity at lower densities are caused by the rapid formation of associated NaCl. Decreases in supercritical water conductivity at higher densities are caused by lower ion mobilities associated with viscosity increases.

The ionic product of water (Kw) is the product of the concentration of hydrogen and hydroxyl ions. At ambient conditions (25°C and 100 KPa), Kw is 10^{-14}. Increases in temperature and pressure alter Kw. At 400°C and 25.0 MPa, Kw is approximately 10^{-19}. Figure 2.5 illustrates Kw vs. temperature at 25.0 MPa.

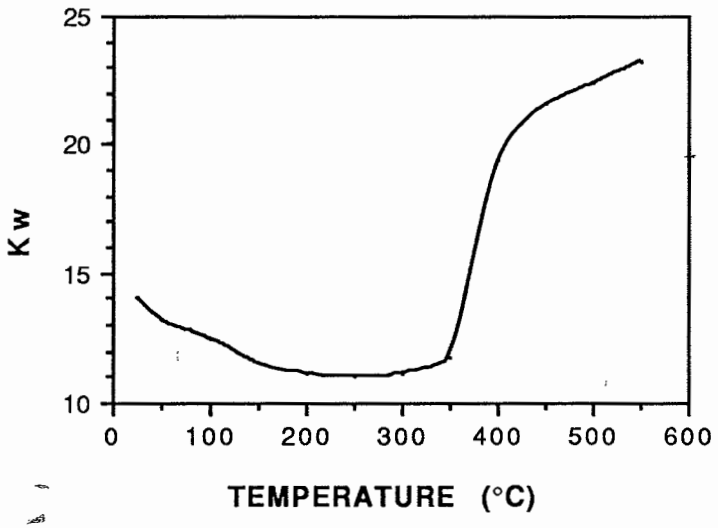

Figure 2.5 Ionic Product of Water at 25.0 MPa
(Dell'Orco, 1991)

2.2 Supercritical Water Oxidation

With the addition of oxygen, supercritical water offers an excellent medium for the total or partial oxidation of organic waste. Organic wastes are oxidized to CO, CO_2, H_2O, H_2, and more refractory lower molecular weight alcohols and volatile acids (Shanableh, 1990; Tongdhamachart, 1990). Organic

nitrogen is oxidized to N_2, NH_3, and NO_3^-. Organic sulfur and phosphorus are oxidized to SO_4^{-2} and PO_4^{-3}. Organic halides are converted to free ions.

SCWO offers several advantages when compared with sub-CWO and WAO (Thomason and Modell, 1984). Organic compounds and oxygen are totally miscible in supercritical water. This characteristic promotes much more efficient mixing and destruction than do sub-CWO and WAO. Smaller reactor volumes are required for the SCWO process, and elevated temperatures and pressures used in SCWO allow for shorter residence times. Lower total energy inputs are necessary, which reduces the cost of waste treatment. Given 3% to 5% organic waste in an influent feed and appropriate heat exchangers, the exothermic release of heat associated with the oxidation of organic carbon and hydrogen may be adequate to maintain reactor temperatures above the critical point of water. Excess heat may be recovered for steam or power generation. At supercritical temperatures and 25.0 MPa, inorganic salts have low solubilities and suspended solids have high settling velocities. These characteristics allow for the highly efficient separation of inorganic salts and suspended solids from the effluent liquid stream.

SCWO has potential as a commercial technology for the treatment of organic waste. Researchers have shown that SCWO is an effective treatment for the destruction of organic liquids, sludges, and slurries (Modell et al., 1982; Shanableh, 1990; Tongdhamachart, 1990; Wilmanns, 1990). However, the mechanism of organic waste destruction by SCWO is not completely understood. A free radical mechanism is believed to be responsible for the high destruction efficiencies (Helling and Tester, 1988; Lee, 1989).

2.3 Behavior of Chromium in Aqueous Systems

Chromium is one of the transition metals of Group VlB in the periodic table. Chromium in aqueous systems occurs in the +3, +4, and +6 oxidation states (Pourbaix, 1976). The dominant oxidation states in aqueous systems are trivalent chromium (Cr^{+3}) and hexavalent chromium (Cr^{+6}). The +4 oxidation state of chromium occurs only at a narrow range of conditions in aqueous systems. When used as a metal alloy, chromium has an oxidation state of zero.

Trivalent and hexavalent chromium form hydrolysis products. Hexavalent chromium hydrolysis products are H_2CrO_4, $Cr_2O_7^{-2}$, CrO_4^{-2}, and

$HCrO_4^-$ (Pourbaix, 1976). The predominate species present is dependent upon the pH of the aqueous system and the concentration of hexavalent chromium. Polymerization of $HCrO_4^-$ to $Cr_2O_7^{-2}$ occurs at a concentration of greater than 0.01 M. Trivalent chromium hydrolysis products are $CrOH^{+2}$, $Cr(OH)_2^+$, and $Cr(OH)_4^-$ (Imai, 1988). The predominate species depends only on the pH of the aqueous system.

Hexavalent chromium does not precipitate with the hydroxyl ion since it exists either as a neutral acid or as an anion. In aqueous systems, hexavalent chromium is almost completely soluble and quite mobile. Trivalent chromium reacts with water to form insoluble chromium hydroxide, $Cr(OH)_3$. Chromium hydroxide transforms slowly to chromium hydrous oxide (Cr_2O_3), which is amorphous and very insoluble in water.

Reactions in which elements undergo changes in oxidation state are referred to as oxidation-reduction reactions. These reactions involve electron transfers and require two half-reactions. The first half-reaction is donation of electrons (oxidation); the second half-reaction is acceptance of electrons (reduction). The oxidation of chromium metal (Cr^0) to trivalent or hexavalent chromium is an example of an oxidation half-reaction. Examples of reduction half-reactions include reduction of H^+ to H_2 and O_2 to H_2O or OH^-.

Trivalent chromium forms soluble salts with acetate, nitrate, sulfate, and halides. Trivalent chromium complexes with carbonates and phosphates have very low solubilities (Brown and LeMay, 1981). Hexavalent chromium hydrolysis products form soluble complexes with the alkali metals and ammonia. Most other complexes of hexavalent chromium hydrolysis products are insoluble (Brown and LeMay, 1981).

Adsorption of soluble chromium species is categorized as anion adsorption for hexavalent chromium and cation adsorption for trivalent chromium. The dispersed solid phase of many wastewater sludges consists predominately of inorganic colloids, such as clays, metal oxides, and metal carbonates, and organic colloidal matter of detrital origin. At the pH values typically encountered in SCWO effluents of wastewater sludges, these colloidal solids will have a negative surface charge. This negative charge is

responsible for adsorption of trivalent chromium to the surface of the colloidal solids.

Both the concentration of such colloidal material in an aqueous system and the pH of the aqueous system itself will determine the distribution of trivalent chromium between the adsorbed and aqueous phases. Higher concentrations of colloidal material and increased pH will shift the equilibrium to the absorbed phase. Similarly, decreases in colloidal material concentration and pH will shift the equilibrium for trivalent chromium to the aqueous phase.

2.4 Generation Of Corrosion Products

Chromium corrosion products generated in SCWO environments are electrochemical in origin. Electrochemical corrosion in SCWO environments is an oxidation-reduction reaction occurring at a metal surface - bulk fluid interface.

Electrochemical corrosion takes place through the action of corrosion cells. Corrosion cells occur when small differences in pH, temperature, and electrolyte concentration arise between very small areas on the same metal surface (Pisigan, 1981). A potential gradient is generated between these areas of differences in pH, temperature, or electrolyte concentration. Areas of lower pH, higher temperature, or lower electrolyte concentration are sites at which chromium metal (Cr^0) is oxidized. These sites are referred to as "anodes." Areas of higher pH, lower temperature, or higher electrolyte concentration are sites at which electron acceptors from the bulk fluid are reduced. These sites are referred to as "cathodes."

Except where localized conditions at the metal surface - bulk fluid interface create stagnant conditions, the pH, temperature, and electrolyte concentration are constantly changing on the metal surface. These changes cause the same surface area to switch periodically between anode and cathode. This results in uniform corrosion of the metal surface (Muzyczko, 1978).

When chromium metal (Cr^0) corrodes, the oxidation half-reaction, as shown in Eq. 2.1, occurs at the anode:

$$Cr^0 \rightarrow Cr^{+n} + ne^- \qquad n = 3 \text{ or } 6. \tag{2.1}$$

The oxidation of chromium metal creates a surplus of electrons at the anode. These excess electrons travel through the metal sub-surface to the cathode under the influence of the potential gradient. At the cathode region of the metal surface - bulk fluid interface, the electrons react with ions and molecules present in the bulk fluid.

In SCWO systems, the predominate reaction at the cathode will be the reduction of O_2 or H^+. One of three reduction half-reactions can predominate at the cathode. The pH of the cathode region will determine which reaction occurs. The possible reactions are:

$$O_2 + 4H^+ + 4e^- \rightarrow 2H_2O \qquad \text{pH 4 to 7} \tag{2.2}$$

$$O_2 + 2H_2O + 4e^- \rightarrow 4OH^- \qquad \text{pH} > 7 \tag{2.3}$$

$$2H^+ + 2e^- \rightarrow H_2 \qquad \text{No } O_2 \text{ present or pH} < 4 \tag{2.4}$$

The pH ranges indicated for Eqs. 2.1, 2.2, and 2.3 are for conditions at which Kw is 10^{-14}. At temperatures and pressures encountered in SCWO systems, Kw can be significantly different. It has not been determined how changes in Kw will affect the pH ranges at which these reactions occur.

The circuit between the anode and cathode is completed by the movement of ions at the metal surface - bulk fluid interface. A balanced oxidation-reduction reaction consisting of Eqs. 2.1 and 2.2 is shown in Figure 2.6. To preserve electroneutrality of the system, the anodic and cathodic half-reactions occur simultaneously and at the same rate.

Electrochemical corrosion can also be explained by Ohm's Law (Uhling, 1971). Due to the presence of potential gradients, the metal surface is composed of many corrosion cells, which are connected by the metal. Ohms Law, as shown in Eq. 2.5, states:

$$I = \frac{E}{R} \tag{2.5}$$

where

I = corrosion current (amps/cm^2),

E = potential between anode and cathode (volts), and

R = total resistance of the metallic circuit (ohms/cm^2).

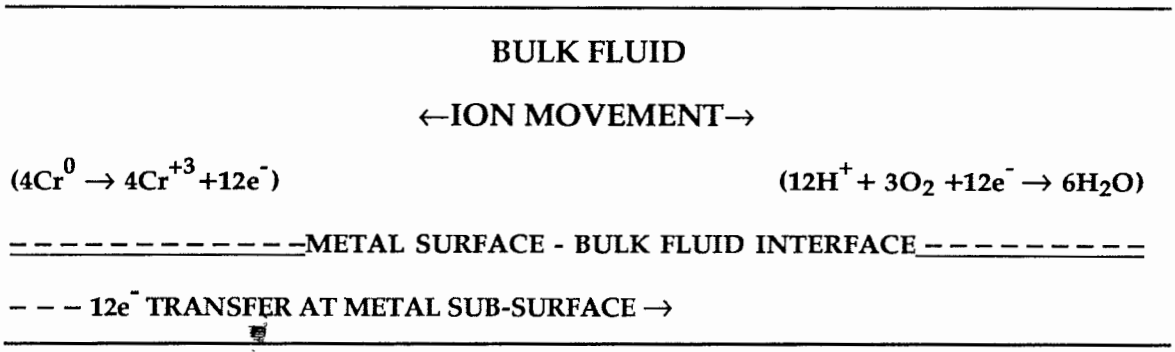

Figure 2.6 Corrosion Of Chromium

Without an electrolyte, significant corrosion will not occur, because the current flow through the metal is lost in heating the metal. However, if an electrolyte is present, corrosion takes place due to the current flow through the electrolyte. The total flow of current in the metal is exactly equal to the total flow of current in the electrolyte (Uhling, 1971). The current in the electrolyte flowing from the anode to the cathode is expressed in Eq. 2.6:

$$I = Ek \tag{2.6}$$

where

k = conductivity of the electrolyte (R^{-1}).

The tendency of chromium metal (Cr^0) to corrode or be oxidized to Cr^{+3} or Cr^{+6} in Cr-H_2O-O_2 systems is related to the free energy of the electrochemical reaction involved. The relationship can be expressed as Eq. 2.7:

$$\Delta G = -nFE \tag{2.7}$$

where

ΔG = Gibbs free energy change (kJ/mole),

n = number of electrons transferred,

F = Faraday's constant (coulombs/electron-mole),

E = electrode potential of corrosion cell (volts).

Eq. 2.7 is a general relationship applicable under all conditions. At standard conditions (25°C and 100 kPa [14.7 psi]) and when reactants and products are at unit activities, Eq. 2.7 is expressed as Eq. 2.8:

$$\Delta G^\circ = -nFE^\circ \tag{2.8}$$

where

ΔG° = standard energy change (kJ/mole) and

E° = standard electrode potential (volts).

A value for either E or E° is essential to determine the free energy change associated with an electrochemical reaction. The oxidation-reduction process will be: (a) spontaneous if ΔG is negative, (b) at equilibrium if ΔG is zero, and (c) not spontaneous if ΔG is positive.

The Nernst equation, shown in Eq. 2.9, describes the equilibrium potential of an oxidation-reduction reaction written as an oxidation reaction (Pisigan, 1981):

$$E = (E^\circ_C - E^\circ_A) + \frac{RT}{nF} \, Ln \frac{\prod\{product\}^x}{\prod\{reactants\}^y} \tag{2.9}$$

where

E	=	corrosion cell potential (volts),
E°_C	=	cathode standard potential (volts),
E°_A	=	anode standard potential (volts),
n	=	number of electrons transferred,
R	=	universal gas constant (1.9872 cal/°C-mole),
F	=	Faraday's constant (23062.4 cal/mole),
T	=	absolute temperature (°K),
{products}	=	activity of oxidation products,
{reactants}	=	activity of reduced species,

x = stoichiometric molar coefficient of products, and

y = stoichiometric molar coefficient of reactants.

For dilute solutions, concentrations and activities of ionic species H^+ and OH^- are almost equal. Concentrations may therefore be substituted for activities. The concentration and activity of H_2O and Cr^0 are "1" by standard convention. The concentration and activity of O_2 and H_2 are expressed in atmospheres of pressure (Stumm and Morgan, 1981).

When using Eq. 2.9, both the anodic and cathodic reactions are written in terms of the reduction reaction. This allows the use of standard reduction potentials published in the literature. Standard electrode potential for some chromium species and O_2 are shown in Table 2.1. As depicted in Eq. 2.10, the reference reaction for these half-reactions is the reduction of hydrogen ion to hydrogen gas at 25°C at 100 KPa (1.0 atm):

$$H^+_{(aq)} + e^- = 1/2H_{2(g)} \text{ where } E° = 0. \quad (2.10)$$

The concentration of H^+ is one activity. This represents the standard hydrogen electrode (SHE).

Table 2.1 Standard Electrode Potentials for Chromium Species and Oxygen
(Weast, 1985)

REACTIONS	E°(volts)
$Cr^{+3} + 3e^- \leftrightarrow Cr^o$	-0.744
$Cr_2O_7^{-2} + 14H^+ + 6e^- \leftrightarrow 2Cr^{+3} + 7H_2O$	1.232
$HCrO_4^- + 7H^+ + 3e^- \leftrightarrow Cr^{+3} + 4H_2O$	1.35
$CrO_4^{-2} + 4H_2O + 3e^- \leftrightarrow Cr(OH)_3 + 5OH^-$	-0.13
$Cr(OH)_3 + 3e^- \leftrightarrow Cr^o + 3OH^-$	-1.48
$O_2 + 4H^+ + 4e^- \leftrightarrow 2H_2O$	1.229
$O_2 + 2H_2O + 4e^- \leftrightarrow 4OH^-$	0.401

2.5 Equilibrium Potential - pH Diagrams

The pH effects are important in understanding the thermodynamics of corrosion in Cr-H_2O-O_2 systems. The thermodynamic treatment of electrode potential coupled with pH effects provides useful information in understanding, predicting, and controlling chromium corrosion. Equilibrium potential - pH graphs (Pourbaix diagrams) combine thermodynamic and pH data into a graphic presentation. Pourbaix diagrams define theoretical conditions of corrosion, immunity, and passivity for a metal.

Construction of Pourbaix diagrams requires thermodynamic data associated with the equilibrium oxidation-reduction reactions and manipulation of the appropriate Nernst equations. The procedure for construction of Pourbaix diagrams is straightforward (Pourbaix, 1976). Computer-assisted calculation and plotting programs have also been developed for the construction of Pourbaix diagrams.

Figure 2.7 is the Pourbaix diagram for a Cr-H_2O-O_2 system at standard conditions. This diagram was generated by Huang et al. (1989a) using a computer-assisted calculation and plotting program. Figure 2.7 is identical to

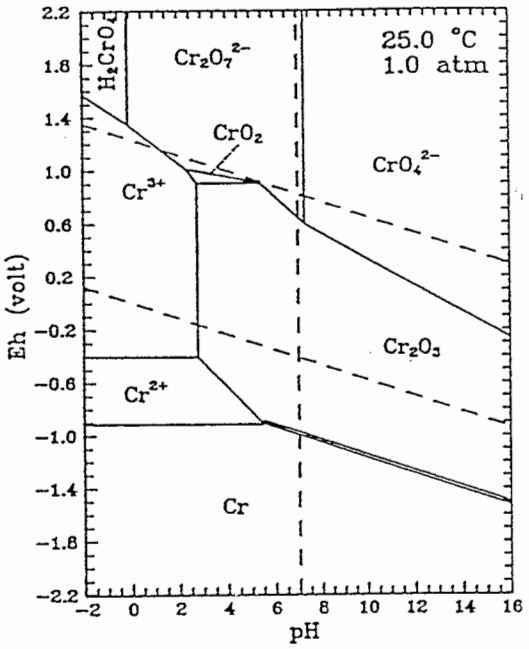

Figure 2.7 Equilibrium Potential - pH Diagram for Cr-H_2O-O_2 System at Standard Conditions (Huang et al., 1989a)

the Pourbaix diagram constructed for Cr-H_2O-O_2 systems at standard conditions by conventional plotting techniques.

The input data for the computer program included temperature, pressure, and chemical data for each chromium species. Chemical data input included activity, standard chemical potential, standard entropy, molecular weight, density, phase state, molecular constituents, charge, and applicable thermodynamic constraints.

The electrode potential, denoted by the Pourbaix diagram Y-axis, is relative to the SHE. In the diagram, a solid line indicates the border between chromium species. This border represents the electrode potential and pH at which equilibrium exists between the chromium species. This line can be horizontal, vertical, or sloping. A horizontal line represents a reaction that is pH dependent but that does not require an electron transfer. A vertical line represents a reaction that requires an electron transfer but that is not pH dependent. A sloping line represents a reaction that is pH dependent and also requires an electron transfer. The vertical dashed line indicates the neutral pH value of water at the given temperature and pressure. The area between the two diagonal dashed lines represents the thermodynamically stable region of water. At electrode potentials above the upper line, water is oxidized to molecular oxygen and hydrogen ion as shown in Eq. 2.11:

$$2H_2O \rightarrow O_2 + 4H^+ + 4e^-. \qquad (2.11)$$

At electrode potentials below the lower line, water is reduced to hydrogen gas and hydroxide ion as shown in Eq. 2.12:

$$2H_2O + 2e^- \rightarrow H_2 + 2OH^-. \qquad (2.12)$$

Figure 2.8 is the Pourbaix diagram for a Cr-H_2O-O_2 system at critical conditions. This diagram was generated by Huang (1989a). An additional routine was developed for the extrapolation of pH values from standard conditions to critical conditions.

Given the desired temperature, pressure, and pH value of the bulk fluid, the routine provided the corresponding pH value and the neutral pH

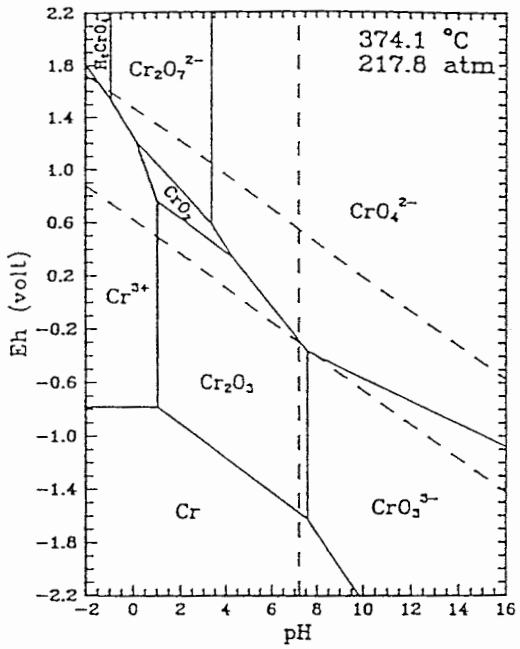

Figure 2.8 Equilibrium Potential - pH Diagram for Cr-H_2O-O_2 System at Critical Conditions
(Huang et al., 1989a)

value at the critical point of water. The equilibrium potential - pH equations for H_2O oxidation and reduction reactions were also provided. These equations determined the upper and lower bounds of the thermodynamically stable region for H_2O at the critical point.

During SCWO of organic waste, the Pourbaix diagram for Cr-H_2O-O_2 systems will not remain constant. The domains of the chromium species will be dependent upon the temperature of the bulk fluid.

The pH of the bulk fluid will also not be constant during SCWO treatment of organic waste. The generation of waste by-products, such as CO_2, organic acids, and ammonia will alter the pH of the bulk fluid. CO_2 and organic acids will lower the pH, whereas ammonia will raise it. Changes in the ionic product of water, associated with temperature increases and decreases of the bulk fluid during heat-up, oxidation, and cool-down, will also alter the bulk fluid pH value.

Certain assumptions are used when applying information derived from Pourbaix diagrams. All reactions involved in the equilibrium potential - pH diagrams are considered to be at equilibrium. The reactions must be known and the thermodynamic data for all solids and metallic ions must be

accurate for the temperature and pressure of interest. It is also assumed that the pH of the reaction regions at the metal surface and the pH of the bulk fluid are equal. This may not be true for a corroding metal surfaces, as the anodic region tends to be more acidic than the cathodic region. It is also assumed that the electrode potential of the corroding metal surface is homogenous. This is not true if crevices or pits are present in the metal surface. Localized electrode potentials in pits and crevices can be significantly higher than at the metal surface.

2.6 Thermodynamic Domains

Pourbaix diagrams are used to determine thermodynamic domains for $Cr\text{-}H_2O\text{-}O_2$ systems. Figures 2.7 and 2.8 identify the pH and electrode potential values at which corrosion, passivity, and immunity domains occur.

In the corrosion domain, the oxidation of chromium metal by O_2 or H^+ generates trivalent chromium or hexavalent chromium hydrolysis products. These chromium species are water soluble, resulting in the continuous generation of chromium corrosion products at the metal surface - bulk fluid interface.

In the passivity domain, the hydrolysis of trivalent chromium generates Cr_2O_3. This results in the formation of a thin protective layer of a water-insoluble oxide film that coats the metal surface - bulk fluid interface. This oxide layer mitigates further corrosion by forming a physical barrier between the bulk fluid and metal surface.

In the immunity domain, the strong affinity of chromium metal for electrons makes chemical reactions between chromium metal and H^+ or O_2 thermodynamically impossible. The inertness of chromium metal at these conditions prevents corrosion.

The Pourbaix diagram for standard conditions (Figure 2.7) illustrates the pH and electrode potential values at which chromium corrosion may occur. Chromium oxide (Cr_2O_3) is the predicted corrosion product for a large part of the region in which water is thermodynamically stable. This oxidation of chromium metal to a water-insoluble corrosion product forms a passivation film over a wide range of pH and electrode potential values.

The Pourbaix diagram for critical conditions (Figure 2.8) shows that chromium oxide (Cr_2O_3) is the predicted chromium corrosion product for only a small part of the region in which water is thermodynamically stable. The oxidation of chromium metal to water-soluble corrosion products occurs over a wide range of pH and electrode potential values. These water-soluble corrosion products are trivalent and hexavalent chromium hydrolysis products.

The predicted passivity domains for Cr-H_2O-O_2 systems are valid only if trivalent chromium complexing agents, such as Cl^- or SO_4^{-2}, are not present in the bulk fluid. If complexing agents are present in low concentrations, the area of the passivity domain can be significantly reduced. High concentrations of complexing agents can eliminate the passivity domain (Pourbaix, 1976).

2.7 Corrosion Kinetics

Pourbaix diagrams are useful in predicting the species of chromium present in aqueous systems at specific pHs and electrode potentials for selected temperatures and pressures. Pourbaix diagrams, however, are not very useful in understanding corrosion kinetics. An understanding of corrosion kinetics gives important insight into predicting the generation rate of chromium corrosion products.

As in other heterogeneous processes (Figure 2.9), the metal surface of a SCWO system in contact with a bulk fluid is covered by a boundary layer of stagnant fluid (Habashi, 1965). Reactants and products exchanged between the bulk fluid and the metal surface must diffuse through this boundary layer. If the reaction rates at the metal surface are faster than the diffusion rates of reactants or products between the metal surface and bulk fluid, the corrosion rate is diffusion-controlled. If the reaction rates are slower than the diffusion rates, the corrosion rate is chemically controlled.

2.7.1 Cathode Reactions and Kinetics

H^+ and O_2 from the bulk fluid are reduced by accepting electrons at the cathode. At a pH of < 4 or if O_2 is absent, H^+ diffuses from the bulk fluid and reacts with electrons at the metal surface where H^+ is reduced to H_2. H_2 then diffuses from the metal surface into the bulk fluid. At a pH of 4 to 7, H^+ and O_2 diffuse from the bulk fluid and react with electrons at the metal surface.

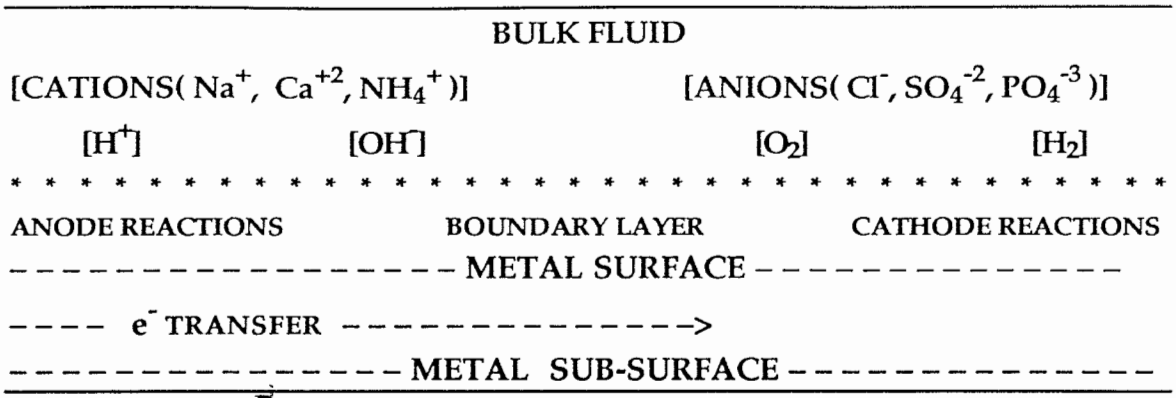

Figure 2.9 Corrosion Environment

O_2 is reduced to H_2O. At a pH > 7, O_2 diffuses from the bulk fluid and reacts with electrons and H_2O at the metal surface. The O_2 is reduced to OH^-. OH^- then diffuses from the metal surface into the bulk fluid.

The recombination reactions involving H^+, electrons, H_2O, and O_2 to form H_2O, H_2, and OH^- require low activation energies. These types of reactions are therefore diffusion-controlled. The reactions at the cathode can exhibit a higher rate of accepting electrons per unit area (electron-moles accepted/cm^2-sec) as compared with the diffusion rate for reactants or products per unit area (reactant or product-moles/cm^2-sec). The maximum reaction rate at the cathode is thus controlled by the rate at which reactants and products diffuse between the bulk fluid and metal surface.

If the pH at the metal surface is < 7 for each mole of electrons donated from the anode, one mole of H^+ is consumed at the cathode. If the pH at the metal surface is > 7 for each mole of electrons donated from the anode, one mole of OH^- is generated at the cathode.

As shown by Eq. 2.13, the maximum corrosion rate at the cathode region for a metal surface exposed to a bulk fluid at a pH < 7 can be obtained by combining diffusion laws (Peron, 1991):

$$i_{Cmax} = \left(\frac{DHAcKcF}{1}\right)\left(\frac{[H^+]_{bulk} - [H^+]_{bound}}{H}\right) \qquad (2.13)$$

where

i_{Cmax} = maximum cathode corrosion current (amps),

A_c = area of cathode region (cm^2),

K_c = velocity constant as 1.0 electron-mole accepted per mole of reactant consumed or product generated,

D_H = diffusion coefficient of H^+ (cm^2/sec),

H = thickness of the boundary layer (cm),

$[H^+]_{bulk}$ = concentration of H^+ in the bulk fluid ($mole/cm^3$),

$[H^+]_{bound}$ = concentration of H^+ in the boundary layer ($mole/cm^3$),

F = 96,487 amps per electron-mole/sec (Faraday's constant).

The maximum corrosion current at the cathode region assuming the pH of the bulk fluid to be > 7, can be expressed by Eq. 2.14:

$$i_{Cmax} = \left(\frac{D_{OH} A_c K_c F}{1}\right)\left(\frac{[OH^-]_{bound} - [OH^-]_{bulk}}{H}\right) \qquad (2.14)$$

where

D_{OH} = diffusion coefficient of OH^- (cm^2/sec),

$[OH^-]_{bulk}$ = concentration of OH^- in the bulk fluid ($mole/cm^3$),

$[OH^-]_{bound}$ = concentration of OH^- in the boundary layer ($mole/cm^3$).

Eqs. 2.13 and 2.14 assume that the volume of bulk fluid in contact with the metal surface has a homogeneous temperature. Differences in temperature will alter pH, diffusion coefficients, and thickness of the boundary layer.

As the temperature of water is increased above 25°C at critical pressures, the dielectric constant of water is lowered. This decrease in the dielectric constant reduces the diffusion rate of H^+ and OH^- between the bulk fluid and metal surface. At a pH of < 7, H^+ may be consumed at a faster rate by the reactions at the cathode than can be supplied by diffusion from the bulk fluid. This reduced diffusion rate of H^+ lowers the reaction rate at the cathode by limiting the electrons-moles accepted per cm^2/sec. At a pH of > 7, OH^- can be generated at a faster rate at the cathode than it can be removed by diffusion from the metal surface to the bulk fluid. This build-up of OH^- lowers the reaction rate at the cathode by reducing the number of reaction

sites available for O_2 reduction. The deficiency of H^+ at a pH of < 7 or the excess of OH^- at a pH of > 7 is referred to as "concentration potential." Generally, concentration potentials in anodic reactions are not rate-limiting processes (Steigerwald, 1968).

At ambient conditions, the low diffusion rate of O_2 from the bulk fluid to the cathode region can result in a reactant deficient concentration potential (Steigerwald, 1968). At low pH ambient conditions, the low diffusion rate of H_2 from the cathode region into the bulk fluid can result in an excess product concentration potential (Muzyczko, 1978).

Oxygen and hydrogen are completely miscible in supercritical water and exhibit very high diffusion rates. The diffusion rates of H_2 and O_2 between the bulk fluid and metal surface will therefore not limit the corrosion current at the cathode.

The thickness of the boundary layer will decrease as the temperature increases. To maintain the mass flow rate at lower fluid densities, which accompany higher temperatures, higher fluid velocities are required. Higher fluid velocities produce larger shear forces that reduce the thickness of the boundary layer (Steigerwald, 1968).

The concentration of H^+ and OH^- in the bulk fluid will be dependent upon the ionic product of water and the dissociation constants of acids and bases in the bulk fluid. Both of these factors are functions of the temperature and density of the bulk fluid.

The differences in concentrations of H^+ and OH^- in the boundary layer and bulk fluid will be significant. At a pH of < 7, H^+ concentrations in the boundary layer will be low, as compared with the H^+ concentration in the bulk fluid, due to the rapid uptake of H^+ at the metal cathode. Conversely, at a pH of > 7, OH^- concentrations in the boundary layer will be high, as compared with the OH^- concentration in the bulk fluid, due to the low diffusion rate of OH^- from the cathode.

2.7.2 Anode Reactions and Kinetics

Chromium metal in contact with an aqueous bulk fluid is initially oxidized to trivalent chromium at the anode. As shown in Eq. 2.15, insoluble

chromium hydroxide $Cr(OH)_3$ is formed upon the hydrolysis of trivalent chromium:

$$Cr^{+3} + 3H_2O \rightarrow Cr(OH)_3 + 3H^+ \quad (2.15)$$

Chromium hydroxide forms chromium oxide (Cr_2O_3), as shown in Eq. 2.16:

$$2Cr(OH)_3 \rightarrow Cr_2O_3 + 3H_2O \quad (2.16)$$

At low pH values, which are related to the temperature and pressure of the environment, $Cr(OH)_3$ dissociates to form Cr^{+3}, as shown by Eq. 2.17:

$$Cr(OH)_3 + 3H^+ \rightarrow Cr^{+3} + 3H_2O. \quad (2.17)$$

As shown in Eq. 2.18, at specific pH and electrode potential values determined by the temperature and pressure of the environment, $Cr(OH)_3$ is oxidized to a hexavalent chromium hydrolysis product:

$$Cr(OH)_3 + H_2O \rightarrow CrO_4^{-2} + 5H^+ + 3e^- \quad (2.18)$$

If complexing agents are present in the bulk fluid, Eqs. 2.19a and 2.19b apply. In this case, $Cr(OH)_3$ dissolves to form trivalent chromium salts.

$$Cr(OH)_3 + 3Cl^- + 3H^+ \rightarrow CrCl_3 + 3H_2O \quad (2.19a)$$

$$2Cr(OH)_3 + 3SO_4^{-2} + 6H^+ \rightarrow Cr_2(SO_4)_3 + 6H_2O \quad (2.19b)$$

Under the above conditions, trivalent chromium ions, hexavalent chromium hydrolysis products, and trivalent chromium salts diffuse from the metal surface into the bulk fluid (Habashi, 1965).

The maximum corrosion rate at the anode can be expressed by Eq. 2.20:

$$i_{Amax} = (E)(k)(A_A) \quad (2.20)$$

where

i_{Amax} = maximum anode corrosion current (amps),

E = potential between the anode and cathode (volts),

k = conductivity of the bulk fluid (ohm^{-1}/cm^2), and

A_A = area of anode region (cm^2).

The potential difference (E) is calculated by the Nernst equation and is dependent upon the potential gradient between the anode and cathode. Electrical conductivity (k) is dependent upon the concentration of disassociated salts in the bulk fluid.

Equation 2.20 assumes that the volume of bulk fluid in contact with metal surface is homogeneous. Differences in temperature and associated salts concentration alter the values of E and k.

2.7.3 Corrosion Rate

The corrosion rate is either diffusion-controlled at the cathode or chemically controlled at the anode. At steady-state conditions, the corrosion current at the anode must equal the corrosion current at the cathode, as shown by Eq. 2.21:

$$i_C = i_A \tag{2.21}$$

$$\text{If } i_{Cmax} > i_{Amax} \text{ then } i_{cell} = i_{Amax} \tag{2.22}$$

$$\text{If } i_{Amax} > i_{Cmax} \text{ then } i_{cell} = i_{Cmax} \tag{2.23}$$

where

i_{cell} = corrosion current (amps).

In SCWO systems, i_{Amax} and i_{Cmax} are dependent upon characteristics of the bulk fluid. Eqs. 2.22 and 2.23 reflect the corrosion current of a metal surface in a SCWO system. Corrosion current can be converted to cm/yr corrosion rate by use of Eq. 2.24 (Muzyczko, 1978):

$$R = \frac{i_{cell} F T M_w}{N P A T} \tag{2.24}$$

where

R = corrosion rate (cm/yr),

i_{cell} = corrosion current (amps),

F = 96,487 amps per electron-mole/sec (Faraday's constant),

T = 3.17×10^7 (sec/yr),

N = number of electrons transferred per atom,

Mw = gms/mole,

P = density (gm/cm^3), and

A = area of metal surface (cm^2).

2.7.4 Effects of Inorganic Salts

Inorganic salts are present in SCWO waste feeds or are generated by the oxidation of organic waste. Inorganic salts, such as NaCl or $CaSO_4$, increase the corrosion rate in SCWO systems (a) by forming strong acids and bases at the anode and cathode, respectively, and (b) by increasing the concentrations of dissociated salts in the bulk fluid (Ahmadi, 1981).

As shown by Eqs. 2.25 and 2.26, strong acids are formed at the anode by these types of reactions:

$$Cr^{+3} + 3H_2O + 3Cl^- \rightarrow Cr(OH)_3 + 3HCl \qquad (2.25)$$

$$2Cr(OH)_3 + 2H_2O + 5SO_4^{-2} \rightarrow 2CrO_4^{-2} + 5H_2SO_4 + 6e^- \qquad (2.26)$$

These reactions lower the pH at the anode and increase the potential gradient between the anode and cathode. The increase in the potential gradient raises the electrode potential and results in higher corrosion currents.

As shown by Eqs. 2.27 and 2.28, strong bases are formed at the cathode by these types of reactions:

$$2Na^+ + 2H_2O + 2e^- \rightarrow 2NaOH + H_2 \qquad (2.27)$$

$$Ca^{++} + 2H_2O + 2e^- \rightarrow Ca(OH)_2 + H_2. \qquad (2.28)$$

These reactions raise the pH at the cathode and increase the potential gradient between the anode and cathode. This increase in the potential gradient and electrode potential results in further increases in the corrosion current.

In addition to increasing the electrode potential between the anode and cathode, dissociated salts also raise the conductivity (k) of the bulk fluid between the anode and cathode. This increase in bulk fluid conductivity increases the corrosion current.

At supercritical temperatures and pressures of ≈ 25 MPa, acids, bases, and salts present in the bulk fluid exist largely as associated species. When acids and bases are associated, the pH at the anode and cathode, respectively, is raised and lowered. Decreases in the difference of the pH value between the cathode and anode reduce the electrode potential and thus decrease the corrosion current. When salts are associated, the conductivity of the bulk fluid between the anode and cathode is reduced. Decreases in bulk fluid conductivity further reduce the corrosion current between the cathode and anode.

2.8 Environmental Regulations

The allowable chromium concentrations in the liquid and solid effluents generated by the SCWO of wastewater sludges are limited by environmental regulations. Chromium concentrations in liquid effluents can be limited by surface water quality considerations and POTW restrictions.

Maximum surface water concentrations of chromium species are regulated by the Clean Water Act. The maximum receiving water concentrations for Texas are shown in Table 2.2.

The maximum concentrations for trivalent chromium in freshwater environments are based upon the hardness of the water. Adsorbed trivalent chromium concentrations in the effluent are factored into soluble trivalent concentration by assuming a partitioning factor that is stream specific. The typical partitioning factor is 3%.

Chromium concentrations in SCWO effluents discharges to POTW systems are regulated. The primary purpose of these regulations is to prevent the concentration of chromium in bio-solids at levels that would interfere with ultimate disposal. As an example, the maximum concentration for

wastewaters discharged to the City of Austin POTW system is 5.0 mg/L total chromium.

Chromium concentrations (as determined by the Toxicity Characteristic Leaching Procedure [TCLP]) of solid effluents generated by the SCWO of

Table 2.2 Chromium Concentration Limits[1]

Species	Acute (ppm)	Chronic (ppm)
Freshwater Environments		
Cr^{+3}	0.8190[Ln(Hardness) + 3.688]	0.8190[Ln(Hardness) + 1.561]
Cr^{+6}	0.016	0.011
Marine Environments		
Cr^{+3}	–	–
Cr^{+6}	1.1	0.050

[1] Texas Administrative Code 31.307, 1992

wastewater sludges will determine the final disposal of these materials. If the TCLP-determined chromium is < 5.0 mg/L, these materials may be disposed of as non-hazardous waste. This would allow placement in a municipal waste landfill.

2.9 Corrosion and Related Studies

The literature related to chromium corrosion and behavior of chromium species at WAO, sub-CWO, and SCWO conditions was reviewed. Review of coupon corrosion and electrochemical corrosion studies provided additional information regarding corrosion rate of chromium-containing alloys at sub-critical and supercritical conditions.

2.9.1 Wet Air Oxidation Studies

Fisher (1971), using batch reactors constructed of chromium-alloy steel, studied the WAO of settled sewage. Although hexavalent chromium appeared in the effluents, its concentration was negligible if one of three conditions existed: (a) the maximum temperature was < 280°C; (b) the pH of

the effluent was mildly acidic, between 5 and 6; or (c) no excess O_2 was available. At 290°C the addition of large excesses of CO_2 to the reactor prior to waste treatment reduced the concentration of hexavalent chromium in the effluent to < 0.1 mg/L. The addition of small volumes (0.25% and 0.50%) of 1.0 N H_2SO_4 to the waste feed prior to treatment also resulted in a hexavalent chromium concentration in the effluent of < 0.1 mg/L.

2.9.2 Sub-CWO and SCWO Studies

Tongdhamachart (1990) treated anaerobically digested municipal sludges by sub-CWO and SCWO. In these tests, the maximum temperatures ranged between 308°C and 458°C; the pressure remained at 25.0 MPa (3600 ± 100 psi), and the flow rates were 50 gm/min and 100 gm/min. A vertical-tube, continuous-flow reactor constructed of Stainless Steel-316 (SS-316) was used. Soluble chromium concentration for all untreated sludges was < 0.5 mg/L. Chromium, however, was present in all liquid fractions of the effluents. The soluble chromium concentration in the liquid effluents ranged from 0.1 mg/L to 3.3 mg/L. Chromium TCLP concentrations for all effluent solids tested were < 1.0 mg/L.

Similarly, Shanableh (1990) subjected industrial excess activated sludge to sub-CWO and SCWO treatment in the same reactor used by Tongdhamachart. Maximum temperatures ranged from 280°C to 458°C. The pressure was maintained at 25.0 MPa (3600 ± 100 psi), and the flow rate was 50 gm/min. Soluble chromium concentration in the untreated sludge was 0.2 mg/L. Chromium was present in the liquid effluents at all temperatures tested. At sub-critical temperatures (< 374°C), the soluble chromium concentrations in the liquid effluent ranged from 1.5 mg/L to 3.4 mg/L. At supercritical temperatures (> 374°C), the soluble chromium concentrations in the liquid effluent ranged from 0.6 mg/L to 2.0 mg/L. Chromium TCLP concentrations for all effluent solids tested were < 0.1 mg/L.

Wilmanns (1992) treated raw Navy sewage "blackwaters" by sub-CWO and SCWO in the same reactor used by Tongdhamachart and Shanableh. Maximum temperatures ranged from 340°C to 400°C. Flow rates ranged from 40 gm/min to 120 gm/min, and pressure was maintained at 3600 ± 100 psi. At supercritical and sub-critical temperatures, soluble trivalent and hexavalent species were removed from the effluent by association and precipitation. At

sub-critical and supercritical temperatures, the hexavalent chromium concentration in the effluent ranged from 0.007 mg/L to 0.02 mg/L. The concentration of trivalent chromium in these effluents at supercritical conditions ranged from 0.11 mg/L to 0.18 mg/L.

Dell'Orco et al. (1993) investigated the separation of sodium salts from supercritical effluents. The occurrence and separation of chromium corrosion products were also investigated. Corrosion in experiments using an oxidant (nitrate or hydrogen peroxide) was chromium selective, whereas in experiments without an oxidant, corrosion appeared non-selective. Chromate was the only chromium corrosion product generated in these experiments. Most chromium corrosion products were recovered as water soluble species. Chromium species were removed from these effluents by association and precipitation in most experiments above 500°C, but were not removed at temperatures near 400°C.

Takashashi et al. (1989) used batch tests to study the sub-CWO and SCWO of human waste. In these studies the reactor was constructed of Hastelloy C-276. Chromium concentrations in the effluents, which were treated at 250°C, 350°C, 400°C, and 500°C for 60 min, ranged from 4 mg/L to 42 mg/L for total chromium and from 2 mg/L to 25 mg/L for soluble chromium. The maximum concentrations for total chromium and soluble chromium occurred at 350°C. Notably, the total and soluble chromium concentrations in the effluents at 400°C and 500°C were approximately 50% less than at 350°C. The total and soluble chromium concentrations at 250°C were < 5.0 mg/L.

Buelow et al. (1990) treated 0.1 M ammonium perchlorate (NH_4ClO_4) and 0.16 M nitromethane (CH_3NO_2) mixtures by SCWO. A continuous-flow reactor constructed of Hastelloy C-276 was used. Three temperatures (400°C, 500°C, and 580°C) and one pressure (38.7 MPa [5575 psi]) were studied. Residence times ranged from 9 sec to 300 sec. Chromium concentrations in nitromethane effluents were < 0.4 mg/L for all test conditions. Conversely, chromium concentrations in ammonium perchlorate effluents ranged from 1.2 mg/L to 4.4 mg/L at 400°C and from 59 mg/L to 130 mg/L at 500°C.

Bramlette et al. (1990) studied the SCWO treatment of surrogate wastes for DOE production facilities and the electronics industry. The DOE surrogate wastes were dilute matrices of $NaNO_3$ and KNO_3 buffered with NH_4NO_3.

The electronics industry surrogate waste was a mixture of 98% water and 2% non-halogenated organics. Inconel-625 and Hastelloy C-276 witness wires were placed in the pre-heater, reactor, and cool-down sections of the reactor. Analyses of witness wires indicated selective and non-selective corrosion of chromium for different treatment conditions and reactor locations.

Hong (1987) studied the SCWO treatment of human waste. A two-stage reactor was used, with maximum temperatures ranging from 608°C to 672°C. Soluble chromium concentrations in the liquid effluents ranged from 3.6 mg/L to 14 mg/L. Chromium concentrations in the solid effluents ranged from 0.03 wt% to 1.2 wt%. The alloy or alloys used in reactor construction were not specified.

2.9.3 Electrochemical Studies

Huang et al. (1989b) investigated the corrosion currents (amp/cm^2) of two chromium alloys (SS-304 and SS-316) at sub-critical and supercritical temperatures. The electrolytes were distilled water and a 0.005 mole/L Na_2SO_4 solution. The oxygen concentration was maintained at < 0.5 mg/L. For both electrolytes, the corrosion currents increased exponentially with temperature up to the critical point then decreased with temperature above the critical point. Corrosion currents for distilled water were less than those for the Na_2SO_4 solution.

2.9.4 Coupon Studies

Matthews (1991) studied the corrosion rate of two chromium alloys (SS-316 and Hastelloy C-276) at sub-critical and supercritical conditions. Three temperatures (300°C, 400°C, and 500°C) and three pHs (2.1, 5.8, and 8.6) were used. The chloride concentration was constant at 420 mg/L. Both alloys experienced higher corrosion rates at 300°C and 500°C, as compared with 400°C, for all pHs tested. Higher corrosion rates were exhibited by coupons exposed to low pHs. The corrosion rate for SS-316 ranged from 0.85 mm/y to 47.90 mm/y. The corrosion rate for Hastelloy C-276 ranged from 0 mm/y to 33.84 mm/y.

Thomas (1990) studied the corrosion rate of 10 chromium alloys during sub-CWO and SCWO treatment of industrial excess activated sludges. Test periods ranged from 67.5 hrs to 106.5 hrs. Maximum temperatures ranged from 292°C to 457°C. The corrosion rates for the 10 alloys ranged from 6

μm/yr to 304 μm/yr. Evaluations of the surface and of the coupons did not reveal selective leaching of chromium from any of the alloys tested.

3.0 MATERIALS AND METHODS

The materials, analytical procedures, and experimental design of this research are presented. Prior research on the behavior of chromium corrosion products in SCWO environments has been largely confined to batch and bench-scale studies. To facilitate a more realistic operational environment, experiments were designed to determine the behavior of chromium species in a continuous-flow, small-scale SCWO pilot plant.

3.1 Sludge Sources And Preparation

Municipal and industrial wastewater sludges were used as waste feeds. The municipal sludge was an anaerobically digested sludge obtained from the City of Austin Hornsby Bend Treatment Facility. The industrial sludge, an excess activated sludge, was collected at its source and shipped to Balcones Research Center, The University of Texas at Austin. These sludges were stored in a cold room at 4°C prior to use.

3.2 Analytical Procedures

All influent and effluent sludges were analyzed according to Standard Methods (Clesceri et al., 1989) or specified EPA procedures. Analyses included pH, chemical oxygen demand, total suspended solids, total soluble chromium, hexavalent chromium, total chromium, acetic acid, chloride, nitrate, sulfate, phosphate, total, volatile and fixed solids, and ammonia. The Quality Assurance Project Plan procedures, prepared for all SCWO projects, were followed to ensure that accuracy and precision requirements were met.

3.2.1 pH

The pH was measured using an Orion Research Digital Ionalyzer, Model 701A. The pH probe was a combination electrode (Fisher No. 13-620-290); precision was ± 0.01 pH units. Operational temperature range was 10°C to 80°C. The pH meter was calibrated prior to each daily use with buffer solutions of pH 4 and 7.

3.2.2 Chemical Oxygen Demand

Chemical oxygen demand (COD) was used to measure the concentration of organic substances in treated and untreated sludges. Dichromate, in a sulfuric acid solution, was used as the oxidizing agent.

Method 5220 D (Closed Reflux, Colorimetric Method, Standard Methods, Clesceri et al., 1989) was used to determine COD. COD measurements of treated and untreated sludge samples provided sludge oxidation data.

The adverse effect of excessive chloride ion and other halides on these measurements was mitigated by complexation with mercuric sulfate. A pre-mixed digestion solution containing dichromate, sulfuric acid, and mercuric sulfate was supplied by the Hach Company. The procedure consisted of transferring two mL of diluted sample aliquot from a representative sample into a vial containing the pre-mixed digestion solution. The sample was then mixed by manually shaking the vial and digesting the contents for 2 hrs at 150°C in a Hach heating bloc. Following digestion the vial was cooled to room temperature and allowed to settle. A spectrophotometer, set at 620 μm, was used to measure light absorption.

COD concentration was based upon colorimetric measurement. Light absorption increases as dichromate (clear yellow) is reduced to trivalent chromium (deep green). The COD concentration was determined by preparing a standard curve of known concentrations (0 to 1000 mg/L). Absorption was plotted against concentration, and a standard curve and formula were developed. COD of the sample was determined by comparing the absorptivity of the sample against the standard curve. A typical COD calibration curve is shown in Figure 3.1.

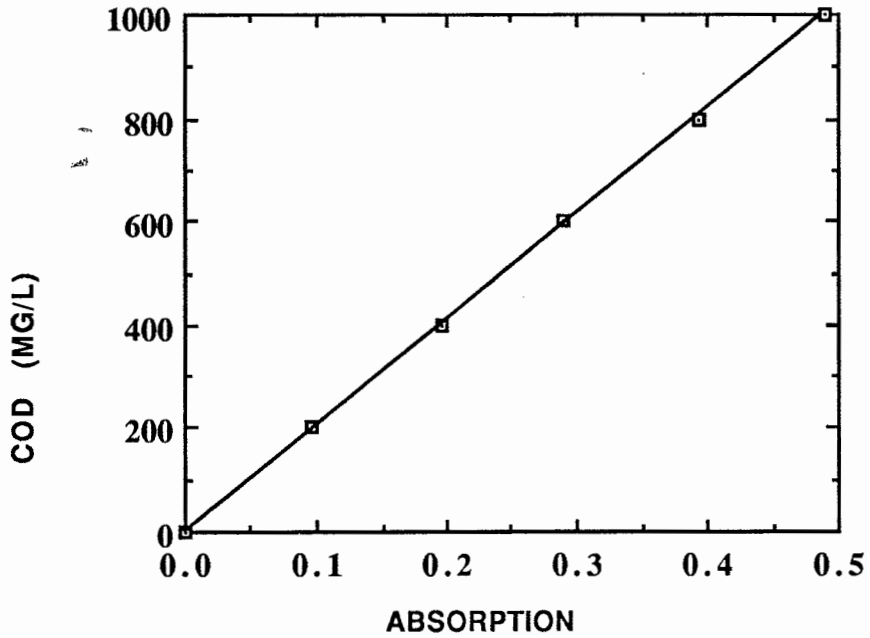

Figure 3.1 COD Calibration Curve

3.2.3 Total Suspended Solids

Total suspended solids (TSS) concentrations were determined by Method 2540 D (Total Suspended Solids Dried at 103-105°C, Standard Methods, Clesceri et al., 1989). A known volume of representative sample was filtered through a tared 0.45 μm filter. The filter paper was dried to a constant weight. Final weight of the filter minus the tare weight of the filter was used to determine mg-TSS/L.

3.2.4 Chromium Analyses

Total chromium, total soluble chromium, and hexavalent chromium analyses were performed. Unless otherwise indicated, soluble chromium measurements were based on the amount that passed through a 0.45-μm filter.

3.2.4.1 Soluble Chromium Species

The total soluble chromium concentration was defined as the sum of the hexavalent chromium and soluble trivalent chromium. Sample filtration and storage for total soluble chromium and hexavalent chromium analyses were performed according to Method 3030 B (Preliminary Filtration, Standard Methods, Clesceri et al., 1989).

Hexavalent chromium was determined by Method 3500-Cr D (Colorimetric Method, Standard Methods, Clesceri et al., 1989). This method utilized the spectral absorption, at 540 μm, of the hexavalent-diphenylcarbazone complex. Absorbance was measured using a Bausch and Lomb spectrophotometer with a 1-cm cuvette. The detection limit was 0.004 mg/L. Analyses were performed by preparing a standard curve of known hexavalent chromium concentration. Absorption was plotted against concentration to provide a standard curve. Hexavalent chromium concentration was determined by comparing the absorption of the sample against the standard curve. A typical hexavalent chromium calibration curve is shown in Figure 3.2.

Total soluble chromium was determined by Method 3111 (Metals by Flame Atomic Absorption Spectrometry, Standard Methods, 1989). Light absorption was set at 362.7 μm. The flame atomic absorption measurements

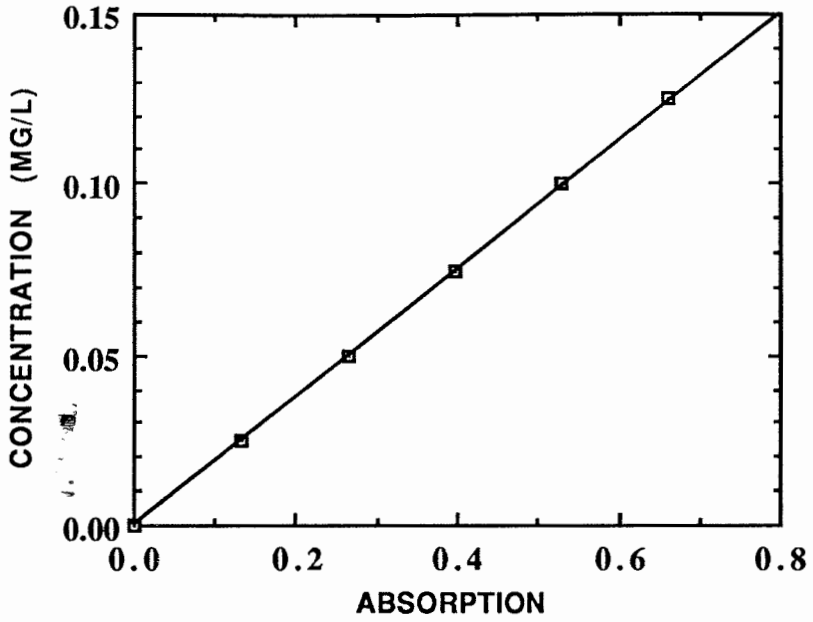

Figure 3.2 Hexavalent Chromium Calibration Curve

were performed with a Perkin-Elmer Model 303, single-head spectrophotometer using air as the auxiliary oxidant and acetylene as fuel. The detection limit was 0.01 mg/L. Analyses were performed by preparing a standard curve of known soluble chromium concentration. A typical total soluble chromium calibration curve is shown in Figure 3.3.

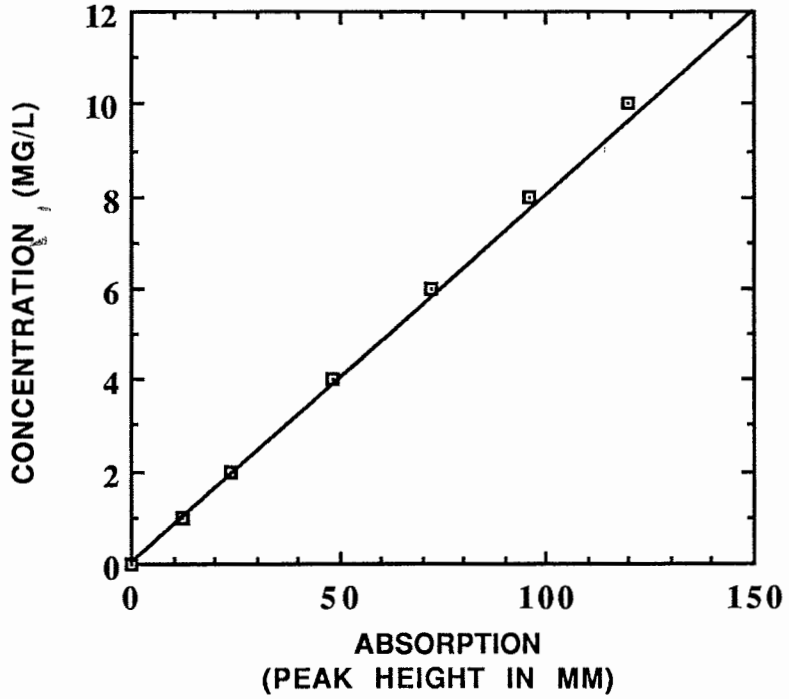

Figure 3.3 Total Soluble Chromium Calibration Curve

Soluble trivalent chromium was determined by subtracting the hexavalent chromium concentration of a sample from the total soluble chromium concentration of the sample. The difference between the concentration of total soluble chromium and hexavalent chromium was the soluble trivalent chromium concentration.

3.3.4.2 Total Chromium

Samples for total chromium determination were prepared by Method 3030 F (Nitric Acid - Hydrochloric Acid Digestion, Standard Methods, Clesceri et al., 1989). A known volume of digested sample was analyzed for total soluble chromium by flame atomic absorption.

3.2.4.3 Insoluble Trivalent Chromium

Insoluble trivalent chromium concentration of samples was determined by subtracting the soluble trivalent chromium concentration from the total chromium concentration.

3.2.5 Anion Analyses

Acetic acid, sulfate, chloride, nitrate, and phosphate concentrations for selected samples were determined by Method 4110 (Determination of Anions By Ion Chromatography, Standard Methods, Clesceri et al., 1989). The analytical equipment consisted of a Dionex System 14 Ion Chromatograph and chart recorder. The chromatograph was equipped with an Ion Pac Column (ASI) and a Pac Guard Column (AGI). The eluent was a solution of DI water containing 0.003 M $NaHCO_3$ and 0.002 M Na_2CO_3. The flow was set at 2.0 mL/min. Anion concentrations of the sample were determined by comparing the peak height of the sample against the peak height standard curves. Figure 3.4 depicts an acetic acid calibration curve. This calibration curve is typical of other anion calibration curves.

3.2.6 Total, Volatile, and Fixed Solids

Total solids (TS) concentrations were determined by Method 2540 B (Total Solids at 103-105°C, Standard Methods, Clesceri et al., 1989). A known volume of sample was dried to a constant weight in a tared crucible. The final weight of the dried sample minus the tared crucible weight provided the concentration of total solids (mg-TS/L).

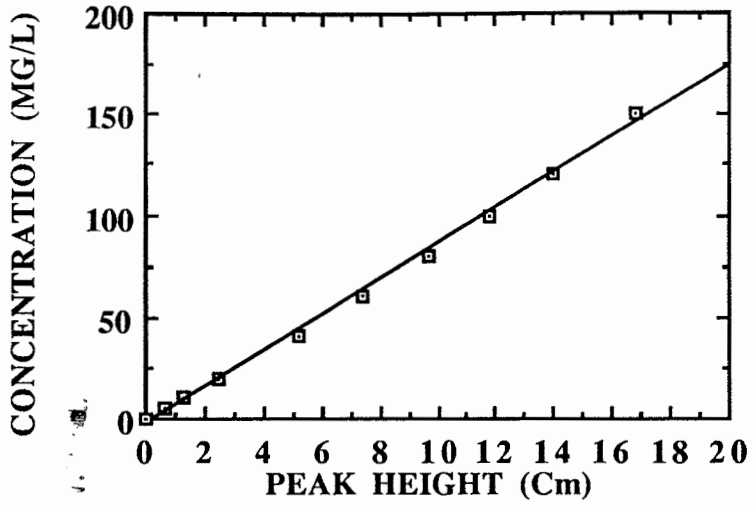

Figure 3.4 Acetic Acid Calibration Curve

Volatile solids (VS) and fixed solids (FS) concentrations were determined by Method 2540 E (Fixed and Volatile Solids Ignited at 550°C, Standard Methods, Clesceri et al., 1989). The residue from Method 2540 B was ignited at 550°C to a constant weight in a tared crucible. The final weight of the ignited sample minus the tared crucible weight provided volatile solids (mg-VS/L) and fixed solids (mg-FS/L) data.

3.2.7 Ammonia

Ammonia concentrations were determined by Method 4500-NH_3 F (Ammonia-Selective Electrode Method, Standard Methods, Clesceri et al., 1989). An Orion Ammonia Selective Electrode, Model 954-12, and an Orion Research Digital Ionalyzer, Model 701A, were used. Measurements in the range of 0.03 mg/L to 1400 mg/L were possible without pre-sample distillation. Measurements were not affected by the color or turbidity of the sample. Ammonia concentrations of the sample were determined by comparing the millivolt response of the sample against a typical calibration curve as shown in Figure 3.5.

3.2.8 Other Metals

Emission spectroscopy was performed with a Hewlett-Packard plasma emission spectrometer. Soluble and total concentrations of sodium, calcium, barium, copper, zinc, and lead were determined for selected samples by Method 3120 B (Inductively Coupled Plasma Method, Standard Methods,

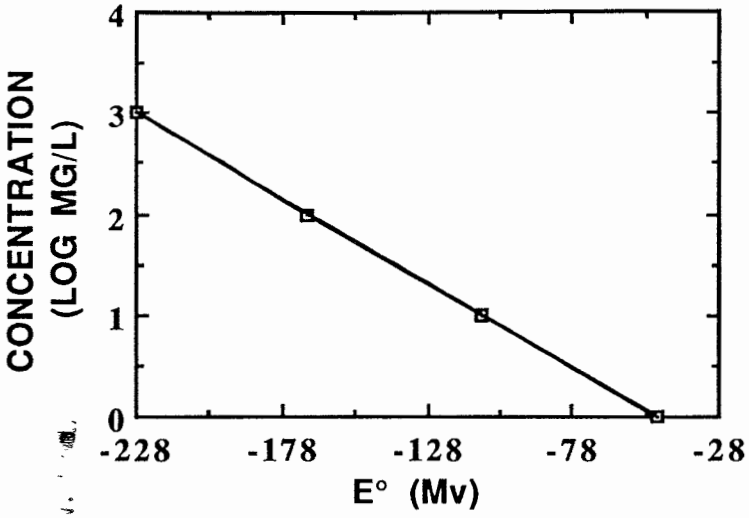

Figure 3.5 Ammonia Calibration Curve

Clesceri et al., 1989). Sample filtration was performed according to Method 3030 B (Preliminary Filtration, Standard Methods, Clesceri et al., 1989). Sample digestion was performed according to Method 3030 F (Nitric Acid - Hydrochloric Acid Digestion, Standard Methods, Clesceri et al., 1989).

3.3 Equipment

A continuous-flow SCWO reactor system was the only type of reactor used for this research. This reactor system was designed to simulate the configuration of a concentric vertical-tube SCWO reactor system. The system was capable of treating liquids, slurries, and sludges.

3.3.1 Continuous-Flow Reactor System

The continuous-flow reactor system included a high pressure pump, a concentric-tube vertical reactor, nine electric band heaters, thermocouples, a pressure gauge/transducer device, weighting scales, control data/acquisition equipment, insulation, and safety shields. Figures 3.6 and 3.7 provide schematics. Tables 3.1, 3.2, 3.3, and 3.4 present system characteristics, dimensions, operating conditions, electric heater spacing, thermocouple locations, and material composition.

The vertical reactor consisted of two concentric tubes constructed of SS - 316. Details are provided in Table 3.1. For these tests, the oxygen injection port was located mid-way in the vertical reactor. The bottom half of

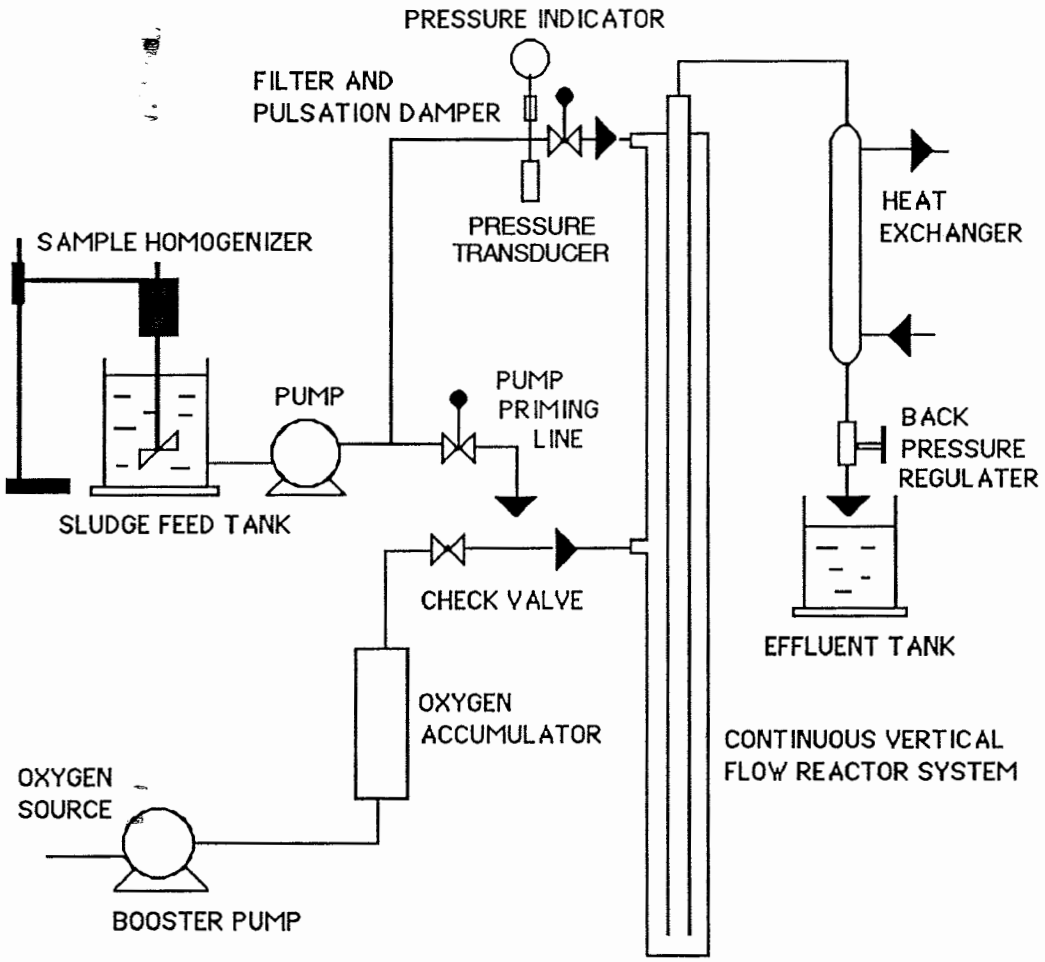

Figure 3.6 Schematic of the Continuous-Flow Vertical-Tube Reactor System
(Shanableh, 1990)

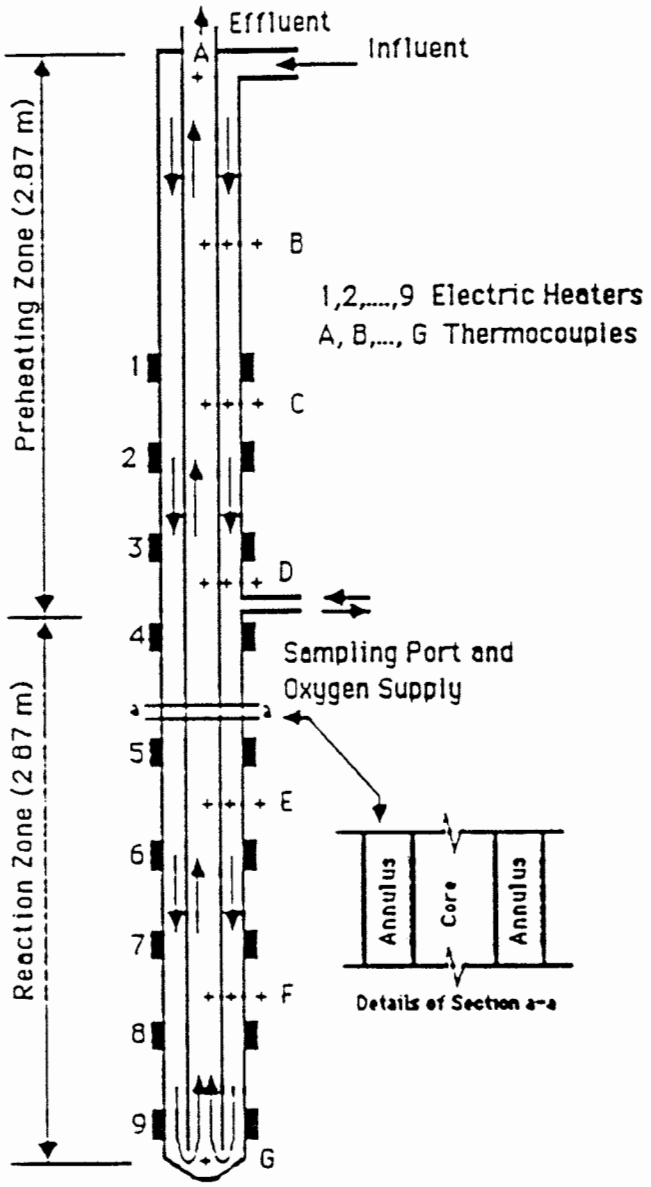

Figure 3.7 Details of the Continuous-Flow Vertical-Tube Reactor
(Shanableh, 1990)

Table 3.1 Characteristics of the Continuous-Flow Reactor System

Item	Detail
Annular Dimensions	5.08 cm O.D. x 2.54 cm I.D. X 5.74 mL
Core Dimensions	0.95 cm O.D. x 0.62 cm I.D. X 5.70 mL
Reactor Volume	2673 cm^3
Flow Rate	10 gm/min to 130 gm/min
Pressure	25.0 MPa (3600 ± 100 psi)
Temperature	450°C maximum
Electrical Heating	9000 watts of power
Oxidant	Analytical Grade Oxygen
Tubes and Fittings	Stainless Steel-316

Table 3.2 Electric Heater Spacing Along the Continuous-Flow Reactor

Heater No.	Distance From Top of Reactor to Top of Heater (m)
1	1.54
2	2.00
3	2.46
4	2.93
5	3.40
6	3.89
7	4.37
8	4.85
9	5.23

Table 3.3 Thermocouple Spacing in the Continuous-Flow Reactor

Thermocouple	Distance From Top of Reactor (m)
A	0.00
B	1.05
C	1.95
D	2.87
E	3.84
F	4.80
G	5.70

Table 3.4 Stainless Steel-316 Material Composition, Continuous-Flow Reactor

Material	Percent Weight
Iron	Balance
Nickel	18.19
Chromium	16.46
Molybdenum	2.11
Copper	0.038
Manganese	1.55
Phosphorus	0.03
Sulfur	0.003
Carbon	0.04
Silicon	0.33

the reactor vessel was considered to be the isothermal reaction zone. Volume of the reaction zone was 1,337 cm^3.

An American Lewa diaphragm pump (Model HLM-1) with a maximum output of 55 MPa (8,000 psi) was used as the feed pump. This pump was capable of handling liquids, sludges, and slurries. Flow rates could be varied from 10 gm/min to 120 gm/min. The maximum particle size that could be handled was 500 μm.

Influent and effluent lines were constructed of SS-316. Fluids in the effluent and sampling lines were cooled by circulating chilled water. The sludge was continuously mixed during pumping to ensure that a homogeneous waste feed was pumped to the reactor.

External heat was provided to the SCWO reactor by nine 1000-watt electric band heaters, Akinsun Model EXB-200600. The heaters were evenly spaced along the length of the reactor. The temperature at thermocouple "G" located inside the bottom core portion of the reactor was used as a feedback device to a temperature controller, Eurotherm Model No. 847. Maximum temperatures were achieved in this section of the reactor. The temperature controller regulated the heat input of the six lower band heaters. The top three heaters were operated manually.

Heat losses at the bottom of the reactor (exterior surface at point "G", Figure 3.7) were minimized by wrapping the flange at this location with electrical heating tape. The temperature of the heating tape was controlled by a rheostat.

As shown in Figure 3.7, the temperature profiles along the external and internal length of the reactor were monitored by seven K-type thermocouples distributed at seven locations. At five of these locations (B-F), thermocouples were located along the outer surface of the reactor piping. At locations A and G, thermocouples were located in the reactor core section. Thermocouples located in the core portions of the reactor were shielded with Inconel-600.

Temperatures of the annular and core fluids along the reactor length were estimated by use of a graph developed by Shanableh (1990). These temperature profiles are shown in Figure 3.8.

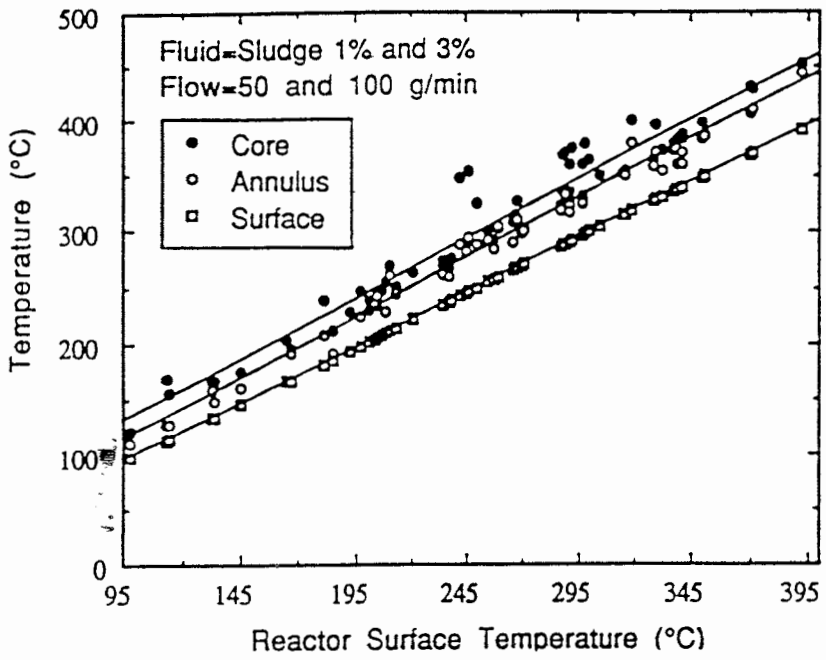

Figure 3.8 Temperatures of Core and Annular Fluids Versus Reactor Surface Temperature
(Shanableh, 1990)

Conductive and convective heat losses were minimized by wrapping the reactor with three layers of ceramic insulation. The first layer was a 2.5-cm-thick layer of Koawool ceramic fiber. The second layer consisted of a 2.5-cm-thick layer of ridged Kaylo pipe insulation. The third layer consisted of an additional 2.5-cm-thick layer of Koawool ceramic fiber. This third layer was restricted to the bottom half of the reactor.

Temperatures and pressures up to 450°C and 27.5 MPa (4,000 psi) were achieved. Pressure in the reactor was regulated by a Whitney RS-4 needle valve. Pressure was monitored by an Ashcroft pressure gauge (10,000 ±50 psi) and a Heise pressure transducer. The gauge was protected by a porous metal fiber, which prevented clogging and reduced pulsation impacts. The pressure transducer interfaced with a Beckman Industrial 600 Series digital readout. A pressure relief valve designed to activate at a pressure of 30.7 MPa (4,500 psig) was used to protect the reactor system. An interconnect, located between the pressure monitoring system and feed pump, was capable of disengaging the feed pump. The cut-off pressure was 27.2 MPa (4,000 psig).

Zero grade bottled oxygen was used as the oxidant. The discharge oxygen pressure was increased to 26.5 MPa (3,900 psig) with a Haskell Model 27267 Gas Booster prior to injection into the reactor system. A Foxboro D/P Cell and a Badger metering valve were used to monitor and regulate the oxygen mass flow. The high pressure oxygen feed was transferred through 0.32 mm O.D. Monel 400 tubing. No special oxygen mixing capability was provided within the reactor. The oxygen line was protected by two in-line check valves. Oxygen to the reactor inlet was controlled by an in-line shut-off valve.

The weight change in the influent tank was determined by an Ohaus, PBI-01-920-44, scale. Mass flow rate (gm/min) of influent was determined and recorded by weight changes in the influent tank.

All gauges and most of the valves were installed on an instrument panel that provided control and monitoring capability for temperature, flow, and pressure. The operator was protected by a 0.64-cm-thick Lexan safety shield.

3.4 Experimental Design

Experiments were designed to determine the concentration and behavior of chromium species generated during the SCWO of wastewater sludges.

Sludge was pumped to the top of the reactor and pre-heated in the annular section prior to being mixed with oxygen at the mid-section of the reactor system. Figure 3.7 provides details.

The influent sludge was pumped downward though the annular space and it then flowed upward through the core section. Heat exchangers were used to quench the effluent. The effluent was depressurized at the effluent collection point and allowed to reach equilibrium with the atmosphere prior to sample collection. Additional sampling ports were located near the middle and at the bottom of the reactor. The sampling collection points were located at the control panel.

Major parameters for this research included temperatures, flow rates, sludge type, and sludge concentration. Five reaction temperatures were used: three in the subcritical range (300°C, 350°C, and 367°C) and two in the

supercritical range (400°C and 450°C). Three different flow rates (60 gm/min, 90 gm/min, and 120 gm/min) were used. The TS of the industrial sludge feed was set at 0.5%. TSS of the anaerobically digested sludge were 0.93% and 1.31%. For these studies the pressure was held at 25.0 MPa (3,600 ±100 psi).

3.5 Operations

Operation of the continuous flow reactor involved the following steps: sludge preparation, reactor pre-heating, sample collection, and reactor cooling and cleaning.

Sludge Preparation: Industrial sludge, adjusted to the desired TS by dilution with distilled water, was prepared and immediately fed to the continuous-flow reactor. Digested municipal sludges were filtered through a 1000 μm sieve and also immediately processed. The influent sludge was continually stirred to ensure a homogeneous feed to the reactor. Samples of the feed were retained for analyses.

Reactor Heating: To initiate the heating cycle, the desired reaction temperature was programmed, and the heaters were turned to the "on" position. During heat-up, distilled water was pumped through the reactor at 120 gm/min. When the desired temperature was reached, sludge was fed to the reactor. Oxygen feed, at a minimum of 200% of stoichiometric demand, was started concurrently with the sludge feed.

Sample Collection: Steady-state conditions were required before effluent samples were collected. A minimum of one reactor volume of influent was pumped to the reactor prior to sample collection. A minimum of two liters of effluent was collected to ensure a representative sample.

Following the collection of the prescribed amount of effluent, the flow was changed. Steady-state flow conditions were achieved and the above sampling procedure was repeated. This procedure was repeated for additional flow rates and temperature settings. During the sample collection phase, the temperature profile was recorded every 30 min.

Grab samples were collected from the bottom sampling port of the reactor at the completion of each sampling run. The volume of this sample was about 50 mL. Selected analyses were performed on these grab samples.

Reactor Cooling and Cleaning: After samples were collected, the heaters were turned off and distilled water was pumped through the reactor. Oxygen feed was continued until the effluent was clear. Distilled water pumping was continued until the reactor bottom temperature dropped below 60°C.

4.0 RESULTS AND DISCUSSION

Data are presented describing the experimental conditions and results derived from the municipal and industrial sludge experiments. Emphasis is directed to chromium speciation and behavior.

4.1 Experimental Conditions

Experimental conditions utilized in these tests are described. The conditions include fluid pathway in the reactor system, temperature profiles, oxygen concentrations, residence times in the vertical-tube reactor, and fluid flow regimes at various experimental conditions.

4.1.1 Reactor System

A pilot-scale, continuous-flow reactor system was used to simulate sub-CWO and SCWO vertical-tube reactor operations. The influent sludge was pumped to the top of the reactor and introduced into the annular section of the reactor at room temperature. The influent sludge flowed downward through the annular section of the reactor. Temperature of the influent sludge was increased by contact with the electrically heated reactor walls. Heating continued until it reached the bottom portion of the reactor. In this lower section, the heated fluid changed direction and flowed upward through the reactor core section; temperature decreased as the fluid flowed upward. The effluent exited the reactor core section and was cooled to ambient conditions by heat exchangers.

4.1.2 Temperature Profiles

Figure 4.1 shows the temperature profiles of the fluid along the length of the reactor for two sub-critical temperatures (300°C and 350°C) and two supercritical temperatures (400°C and 450°C). These temperature profiles were developed during the sludge treatment tests.

4.1.3 Oxygen Concentrations

Oxygen was introduced in the annular section of the reactor at a point 3.0 m below the top of the reactor. Therefore, in the heat-up section, there was little oxidation of organic materials. The control system delivered oxygen to the sludge at significantly higher levels than the stoichiometric demand.

For example, 0.17 lb/hr of oxygen was required for the municipal sludge influent for a COD of 10,500 mg/L and a flow rate of 120 gm/min. During these tests, the oxygen control system was regulated to provide a flow rate of 0 to 6 lb/hr. The 0.17 lb/hr oxygen requirement was below the controllable range for the system (1.0 lb/hr). This excess oxygen translated to approximately 600% of the stoichiometric demand.

For the industrial sludge tests, the control system was modified to regulate a flow rate of 0 to 35 lb/hr. According to calculations, 0.08 lb/hr of oxygen was required for a COD of 5,000 mg/L and a flow rate of 120 gm/min. This oxygen flow rate requirement was also below the controllable range for the system (0.5 lb/hr). A 0.5 lb/hr oxygen flow rate translated to 625% of the stoichiometric oxygen demand. At flow rates of 90 gm/min and 60 gm/min, respectively, the excess oxygen was approximately 975% and 1350% of the stoichiometric demand.

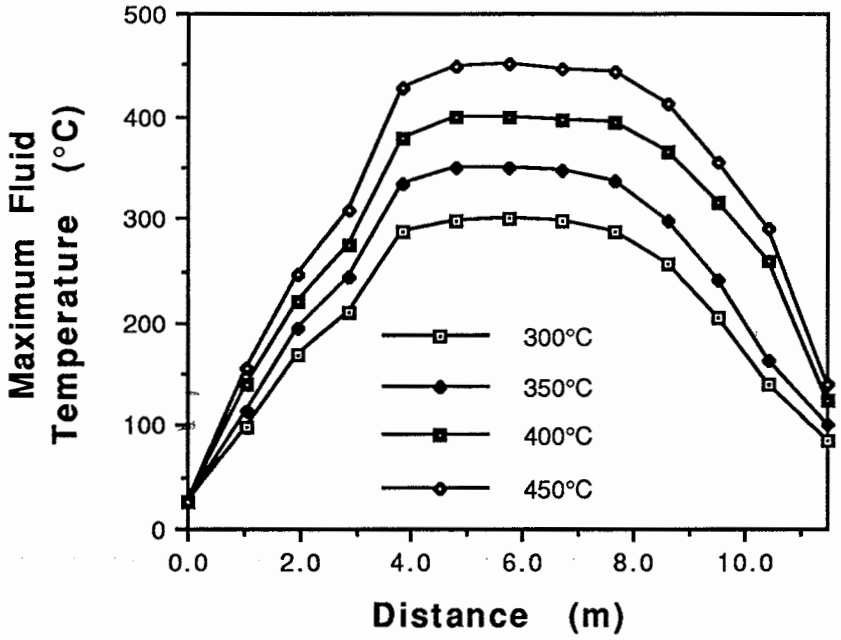

Figure 4.1 Effluent Temperature Profiles

4.1.4 Residence Times

The total residence time of the sludge effluent in the continuous-flow reactor was dependent upon the maximum temperature setting and pumping rate. It was difficult to predict the total residence time of the sludge effluent

due to a non-isothermal profile along the reactor length. However, as shown in Figure 4.1, a relatively constant temperature profile was achieved in the lower sections. This "reaction zone" occurred from 3.84 m to 7.68 m along the annular and core sections.

The total residence time of the effluent in the reaction zone was estimated by dividing the reaction zone volume by the volumetric flow rate. Volumetric flow rates at different reaction temperatures were calculated from the known mass flow rates and pressure-temperature density data for water (Gallanger and Haar, 1985) and oxygen (Sychev et al., 1987).

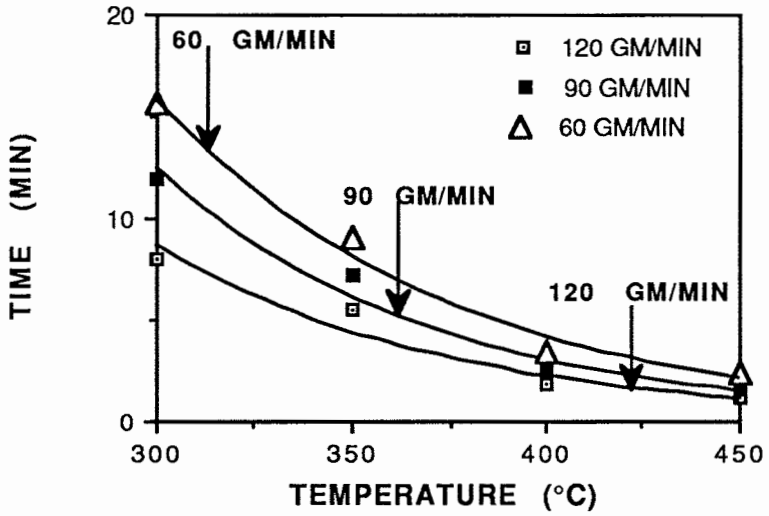

Figure 4.2 Reaction Zone Residences Times

At a constant mass flow rate, the residence time in the reaction zone decreased as the temperature increased. Higher fluid velocities were required to maintain mass flows at the lower fluid densities associated with higher temperatures. Figure 4.2 shows residence times in the reaction zone based upon three flow rates (60 gm/min, 90 gm/min, and 120 gm/min), two sub-critical water temperatures (300°C and 350°C), and two supercritical water temperatures (400°C and 450°C).

4.1.5 Flow Regimes

Flow regimes in the reaction zone were dependent upon the fluid temperature and the influent pumping rate. The Reynolds numbers for maximum flows and higher fluid temperatures were in the low-turbulent

range. Conversely, lower temperature fluids and reduced pumping rates were characterized by Reynolds numbers in the transition and laminar ranges. Table 4.1 shows the Reynolds numbers for fluids in the annular and core sections of the reaction zone for various temperatures and flow rates. These data are based upon known mass flow rates and density and viscosity values for water at 25.0 MPa (3209 psi) (Gallanger and Haar, 1985).

Table 4.1 Reynolds Numbers

Temperature (°C)	Flow Rate (gm/min)	Core	Annulus
450	120	8072	3999
450	60	4036	2000
400	120	8012	3969
400	90	6009	2977
400	60	4006	1985
350	120	3211	1591
350	60	1605	795
300	120	2549	1263

4.2 Municipal Sludge Results

Two runs, one sub-critical and one supercritical, were made utilizing municipal sludge. In this case, the temperature and flow rate were held constant. The sub-critical and supercritical temperatures were 300°C and 400°C, respectively. The flow rate for both runs was 120 gm/min. The calculated residence times for the 300°C and 400°C runs, respectively, were 7.9 and 1.8 min. The total mass of sludge pumped to the reactor was approximately 8.8 kg for both test runs. Tables 4.2 and 4.3 summarize the conditions and results for these runs.

4.2.1 pH

At a fluid temperature of 300°C, pH increased from 7.3 (influent) to 7.9 (effluent) and at 400°C, pH increased from 7.4 to 7.9. The pH of the effluent, as compared to the influent, increased as a result of NH_3 production. NH_3 was

Table 4.2 Summary of Anaerobic Digester Sludge Treated at 300°C

Parameter	Influent	Bottom	Effluent
Total Chromium (mg/L)	0.40	1.36	0.76
Total Trivalent Chromium (mg/L)	0.40	1.32	0.71
Total Soluble Chromium (mg/L)	<0.01	0.74	0.44
Hexavalent Chromium (mg/L)	<0.004	0.035	0.046
Soluble Trivalent Chromium (mg/L)	<0.01	0.71	0.39
Nonsoluble Trivalent Chromium (mg/L)	0.40	0.62	0.32
Nonsoluble Trivalent Chromium (mg/kg)	43	138	86
Total Suspended Solids (gm/L)	9.2	4.5	5.5
Chemical Oxygen Demand (mg/L)	10200	970	2300
pH	7.3	7.8	7.9
Ammonia (mg/L)	94	190	661
Chloride (mg/L)	200		215
Acetic Acid (mg/L)	375		2050

Table 4.3 Summary of Anaerobic Digester Sludge Treated at 400°C

Parameter	Influent	Bottom	Effluent
Total Chromium (mg/L)	0.54	6.13	0.77
Total Trivalent Chromium (mg/L)	0.54	5.84	0.77
Soluble Trivalent Chromium (mg/L)	<0.01	3.71	0.16
Hexavalent Chromium (mg/L)	<0.004	0.288	<0.004
Nonsoluble Trivalent Chromium (mg/L)	0.54	2.13	0.61
Nonsoluble Trivalent Chromium (mg/kg)	41	56	110
Total Suspended Solids (gm/L)	13.1	37.5	5.5
Chemical Oxygen Demand (mg/L)	11300	1100	2600
pH	7.4	7.7	7.9
Ammonia (mg/L)	98	200	419
Chloride (mg/L)	233	140	237
Acetic Acid (mg/L)	490	<50	1500

produced by the oxidation of organic nitrogen. At 300°C, the NH_3 concentration increased from 94 mg/L (influent) to 661 mg/L (effluent). Similarly, at 400°C the NH_3 concentration increased from 98 mg/L to 419 mg/L.

However, the impact NH_3 had on pH was partially counteracted by the formation of acetic acid. The acetic acid concentration in the 300°C test increased from 375 mg/L (influent) to 2,050 mg/L (effluent). The 400°C test showed an increase of acetic acid from 490 mg/L to 1,500 mg/L.

4.2.2 Total Suspended Solids Reduction

During sub-CWO and SCWO of these sludges, the TSS concentration was reduced by the destruction of organic solids. The 300°C and 400°C runs achieved similar levels of TSS reduction. The TSS concentrations in the higher and lower temperature tests were 60% and 58%, respectively. The remaining suspended solids consisted of clay, sand, insoluble inorganic salts, and metal oxides.

The TSS concentrations in the reactor bottoms collected at the completion of the 300°C and 400°C runs were 4.5 mg/L and 37.2 mg/L, respectively. The higher concentration of suspended solids in the 400°C sample, as compared with the 300°C sample, was due to the higher settling rate at the higher temperature. Under supercritical conditions, this higher settling rate was attributable to both lower density and lower viscosity of the fluid. At 400°C, in contrast to 300°C, the settling velocity of the suspended solids increased by a factor of four.

4.2.3 Chemical Oxygen Demand Reduction

The COD reduction in both the 300°C and 400°C runs was similar (77% to 78%). The equivalent degree of COD reduction in the 300°C run resulted from the longer reactor residence time. The residual COD measurement was mostly due to thermal stability of acetic acid at temperatures of < 450°C.

4.2.4 Influent Sludge

The total chromium concentrations in the influent sludge for the 300°C and 400°C runs were 0.40 mg/L and 0.54 mg/L, respectively. Nonsoluble trivalent chromium was the only chromium species detected. Trivalent chromium contained in the influent sludges was adsorbed to the

surfaces of inorganic particulates, such as metal carbonates, clays, and metal hydroxides.

The differences in the total chromium concentrations resulted from variations in TSS concentrations. The 300°C and 400°C test sludges contained 9.3 TSS-mg/L and 13.1 TSS-mg/L, respectively. The concentrations of solids-bound chromium were 43 mg-Cr^{+3}/kg-TSS for the 300°C influent sludge and 41 mg-Cr^{+3}/kg-TSS for the 400°C influent sludge. These are relatively low chromium concentrations for digested municipal sludges. The median chromium concentration for these type of sludges is 500 mg/kg-TSS (Metcalf and Eddy, 1991).

4.2.5 Effluent Characterization

The concentrations of total chromium in the effluents were similar for the two temperatures: 0.76 mg/L for 300°C and 0.77 mg/L for 400°C. Increases in the total chromium concentrations were 0.36 mg/L and 0.23 mg/L for 300°C and 400°C, respectively.

There were significant differences in the total chromium concentrations in samples collected from the reactor bottoms. At 300° and 400°C these concentrations were 1.4 mg/L and 6.1 mg/L, respectively. The higher concentration in the 400°C bottom sample reflected the greater removal rates of chromium species from the effluent at supercritical vs. sub-critical conditions.

Comparison of increases in total chromium concentrations resulting from the generation of chromium corrosion products was not attempted. The retention of trivalent and hexavalent chromium corrosion products in the reactor bottoms made this type of material balance impractical.

4.2.6 Nonsoluble Trivalent Chromium

The concentrations of nonsoluble chromium were comparable between the influents and effluents for both runs. Nonsoluble trivalent chromium concentrations in the 300°C influent and effluent were 0.40 mg/L and 0.32 mg/L, respectively. For the 400°C run, the influent and effluent concentrations were 0.54 mg/L and 0.61 mg/L, respectively. These comparable concentrations between the influent and effluent suggest that: (1) the particulates containing adsorbed trivalent chromium were not being

retained in the bottom portion of the reactor and (2) adsorbed trivalent chromium was not moved from the solid phase to the liquid phase.

The fraction of nonsoluble trivalent chromium in the effluents derived from the two different temperatures was markedly different. At 400°C, 79% of the total trivalent chromium was nonsoluble. At 300°C, however, only 45% of the total trivalent chromium was nonsoluble. This higher percentage of nonsoluble trivalent chromium in the 400°C effluent resulted from the retention of soluble trivalent chromium during the 400°C test at a higher rate than during the 300°C test.

The destruction of organic solids contained in the influent was reflected in the higher trivalent chromium concentration of the effluent dry solids as compared to the influent. In the 300°C and 400°C effluents, the nonsoluble trivalent chromium concentrations increased from 43 mg/kg-TSS to 86 mg/kg-TSS and from 41 mg/kg-TSS to 110 mg/kg-TSS, respectively.

The concentrations of nonsoluble chromium in the bottom portion of the reactor at completion of the 300°C and 400°C runs were 0.6 mg/L and 2.1 mg/L. The higher concentration of nonsoluble chromium species in the 400°C bottom sample is an indication of the higher removal rates of nonsoluble chromium species at 400°C vs. 300°C.

The removal of soluble trivalent chromium corrosion products from these effluents as insoluble chromium compounds, such as $Cr(OH)_3$, $Cr_2(CO_3)_3$, and $CrPO_4$ or adsorbed trivalent chromium, was minimal. At 400°C and 25.0 MPa (3,209 psi), the Kw of water and Ksp of $Cr(OH)_3$ are approximately 10^{-19} and 6.1×10^{-35}, respectively. Calculations showed that at these conditions only a very small amount of $Cr(OH)_3$ would be precipitated from a dilute (<1 mg/L) soluble trivalent chromium solution.

The concentrations of Ca and Cr, respectively, in the solid phase of the 400°C bottom sample were 4,200 mg/L and 2.1 mg/L. Given this large concentration difference, it was assumed that soluble trivalent chromium was removed as an impurity from this effluent by co-precipitation with possibly $CaCO_3$ and $Ca_3(PO_4)_2$. When co-precipitation occurs, normally soluble ions are carried from the solution concurrently with the precipitation of insoluble salts. The Ksp values for $CaCO_3$ and $Ca_3(PO_4)_2$, respectively, are 2.8×10^{-9} and 2.0×10^{-29}. These salts are relatively insoluble at ambient

conditions. Therefore, it was assumed that co-precipitated soluble trivalent chromium remained in this insoluble salt matrix as an impurity, and it was reported as a nonsoluble chromium species.

Adsorption of cations to the surfaces of inorganic particulates was not considered. Adsorption is a relatively slow process. Therefore, adsorption of soluble trivalent chromium corrosion products onto the surfaces of settled particulates in the reactor bottom sediments was assumed to be relatively insignificant.

4.2.7 Soluble Trivalent Chromium

The concentrations of soluble trivalent chromium in both influent sludges were < 0.01 mg/L. Soluble trivalent chromium concentrations in the 300°C and 400°C effluents, respectively, were 0.39 mg/L and 0.16 mg/L. Conversely, the concentrations of soluble trivalent in the 300°C and 400°C bottom samples were 0.71 mg/L and 3.71 mg/L, respectively. The higher concentration in the 400°C bottom sample resulted from the increased removal of soluble trivalent chromium in an associated soluble salt matrix from the 400°C effluents, as compared to the 300°C effluents.

The soluble trivalent chromium salts, which are typically present in digested municipal sludge SCWO effluents, are shown in Table 4.4. Relative solubilities and Ksp values at an ionic strength of zero, if available, are included.

Table 4.4 Solubility Data For Trivalent Chromium Salts at Ambient Conditions [2]

Salt	Solubility	Ksp
$Cr(CH_3COO)_3$	246 mg/L	3.2×10^{-10}
$Cr(NO_3)_3$	High Solubility	NA
$CrCl_3$	67,000 mg/L	8.9×10^{-1}
$Cr_2(SO_4)_3$	50,000 mg/L	3.5×10^{-3}

[2] Sillen and Martell, 1964

The concentrations of these soluble trivalent salts and other selected species were determined in the 400°C filtered sediment bottom sample. These data are presented in Table 4.5.

The low concentrations of CH_3COO^- and NO_3^-, as compared with $SO4^{-2}$ and Cl^-, were predictable. Acetic acid is a weak acid at ambient conditions. The Ksp and pK values for acetic acid are 1.76 X $1O^{-5}$ and 4.75. Thus, at ambient conditions, acetic acid is dissociated in these effluents to CH_3COO^- and H^+. However, at supercritical conditions, weak acids are associated and exist as organic compounds. At these associated conditions, the acetate anion would not be available to precipitate Cr^{+3} and other cations.

Salts containing NO_3^- are more soluble than salts containing Cl^- and SO_4^{-2}. Also, the concentration of NO_3^- in SCWO effluents derived from digested municipal sludges ranges from only 25 mg/L to 50 mg/L (Tongdhamachart, 1990). Therefore, it was not unexpected to find NO_3^-

Table 4.5 Concentration of Selected Species in 400°C Filtered Bottom Sample

Species	Concentration (mg/L)	Concentration (gm-mole/L)
Cr^{+3}	3.71	7.1×10^{-5}
CH_3COO^-	<50	$<8.8 \times 10^{-4}$
NO_3^-	<50	$<8.1 \times 10^{-4}$
Cl^-	140	3.9×10^{-3}
SO_4^{-2}	1700	1.8×10^{-2}
Ca^{+2}	280	7.0×10^{-3}
Na^+	153	3.8×10^{-3}
Σ Anion Equivalents (as HSO_4^- only)		1.8×10^{-2}
Σ Cation Equivalents (as Ca^{+2} plus Na^+)		1.8×10^{-2}

concentrations in the reactor bottom samples to be < 50 mg/L. Given these conditions, removal of soluble trivalent chromium from this effluent by association and precipitation of $Cr(CH_3COO)_3$ and $Cr(NO_3)_3$ was neither expected nor detected.

Concentrations of SO_4^{-2} and Cl^- followed the solubility rules for salts containing these anions. SO_4^{-2} salts are much less soluble than Cl^- salts at 400°C and 25.0 MPa. The solubilities of $CaCl_2$, NaCl, Na_2SO_4 and $CaSO_4$ at these conditions are approximately 10 ppm, 600 ppm, 1.0 ppm, and 0.03 ppm (Martynova, 1976). These large solubility differences resulted in the precipitation of SO_4^{-2} salts rather than Cl^- salts.

Removal of SO_4^{-2} from the supercritical fluid was largely due to the association and precipitation of $Ca(HSO_4)_2$ and $NaHSO_4$. At ambient conditions and at a pH of > 1.81, HSO_4^- dissociates to form SO_4^{-2} and H^+. The dissociation constant is 1.2×10^{-2}. However, at the test conditions, due to the low concentrations of OH^-, SO_4^{-2} was expected to have been present as HSO_4^-. At 350°C and 25.0 MPa, the dissociation constant of HSO_4^- is 3.0×10^{-7} (Marshall, 1976). At 25.0 MPa, the Kw decreases from 10^{-12} to 10^{-19} as the temperature is raised from 350°C to 400°C. At these conditions the dissociation constant of HSO_4^- would be approximately 3.0×10^{-14}. These results were verified by the experimental anion-cation balance. Table 4.5 shows that the summations of anion equivalents (as HSO_4^- only) and cation equivalents (as Ca^{+2} plus Na^+) are equal.

Association and precipitation of other soluble SO_4^{-2} salts did not play a significant role in the removal of SO_4^{-2} from the 400°C effluent. For example, $(NH_4)_2SO_4$ has a higher solubility and a larger Ksp than Na_2SO_4. Therefore, the SO_4^{-2} would precipitate with Na^+ rather than NH_4^+. The solubility and Ksp of K_2SO_4 are similar to Na_2SO_4. However, the concentration of Na^+ in these effluents was significantly greater than the concentration of K^+. $BaSO_4$ and $MgSO_4$ have solubilities and Ksp values in the same range as $CaSO_4$. However, the concentrations of the Ba^{+2} and Mg^{+2} were low relative to the Ca^{+2} concentration in this effluent.

The build-up of soluble trivalent chromium in the bottom portion of the reactor resulted from its co-precipitation, as an impurity, with $Ca(HSO_4)_2$ and $NaHSO_4$. This conclusion was based upon: (a) the lower Ksp for $CaSO_4$ as

compared with $Cr_2(SO_4)_3$ and (b) the much higher concentrations of Ca^{+2} and Na^+ in the filtered bottom sample as compared with Cr^{+3}. The Ksp of $CaSO_4$ (3.7×10^{-9}) at the test conditions was lower by approximately two orders of magnitude as compared with the Ksp of $Cr_2(SO_4)_3$ (3.5×10^{-7}). Similarly, the molar concentrations of Ca^{+2} and Na^+ were higher by two orders of magnitude as compared with the Cr^{+3} concentration.

The concentration of Cl^- in the effluent was approximately 200 ppm. Given the relatively high solubility of Cl^- salts as compared with SO_4^{-2} salts, it was assumed that Cl^- was also removed from the effluent as an impurity by co-precipitation with $Ca(HSO_4)_2$ and $NaHSO_4$.

At ambient conditions, the associated $Ca(HSO_4)_2/NaHSO_4$ salt matrix dissociated to form soluble anions and cations (Ca^{+2}, Na^+, H^+, and SO_4^{-2}). The Cl^- and Cr^{+3} ions present as co-precipitates in this associated soluble salt matrix thus returned to the soluble phase.

4.2.8 Hexavalent Chromium

Hexavalent chromium behaved differently under supercritical conditions as compared with subcritical conditions. Hexavalent chromium salts were not removed by association and precipitation from the 300°C tests. The concentrations of hexavalent chromium in the effluent and bottom samples were 0.046 mg/L and 0.035 mg/L, respectively. Thus, there was no retention mechanism for hexavalent chromium in the reactor bottoms.

As opposed to sub-critical conditions, hexavalent chromium was removed very effectively from the supercritical effluents by association and precipitation of hexavalent chromium salts. The concentrations of hexavalent chromium in the 400°C effluent and bottom samples were < 0.004 mg/L and 0.288 mg/L, respectively. This change in the behavior of hexavalent chromium at supercritical conditions, as compared with subcritical, was not expected. At 25.0 MPa, the solubility and Ksp values for salts are very different at 400°C as compared to 300°C. The solubility of salts can be reduced by as much as three orders of magnitude at the higher temperature. At these conditions, the Kw at 300°C and 400°C are 10^{-12} and 10^{-19}, respectively. This reduction in the Kw at 400°C lowered the Ksp value for salts by seven orders of magnitude.

Table 4.6 provides solubility data for some of the more likely hexavalent chromium salts. Included are the solubilities, or relative solubility, of these hexavalent chromium salts at ambient conditions. If available, the Ksp value for a solution at an ionic strength of zero is included.

Hexavalent chromium association and precipitation as Pb^{+2}, Ba^{+2}, Cu^{+2}, and Zn^{+2} chromate salts was expected in these effluents. These hexavalent chromium salts have low solubilities at ambient conditions; their solubilities at supercritical conditions are expected to be low enough that they would be removed from the effluent by association and precipitation to concentrations of < 0.004 mg/L. Conversely, Na^{+}, Ca^{+2}, K^{+}, and NH_4^{+} hexavalent chromium salts have high solubility at ambient conditions. It was assumed that the solubility and Ksp values of these salts would be large enough at supercritical conditions to reduce the likelihood of removal by association and precipitation. This assumption was based on previous research (Dell'Orco et al., 1993). In previous separation studies utilizing sodium salts at supercritical conditions, the concentration of sodium chromate in the effluent did not decrease until the temperature was greater than 500°C.

Table 4.6 Solubility Data for Hexavalent Chromium Salts at Ambient Conditions [3]

Salt	Solubility	Ksp
$(NH_4)_2CrO_4$	405,000 mg/L	NA
$CaCrO_4$	182,000 mg/L	7.1×10^{-4}
Na_2CrO_4	870,000 mg/L	NA
K_2CrO_4	629,000 mg/L	2.7×10^{-1}
$BaCrO_4$	4.4 mg/L	1.2×10^{-10}
$PbCrO_4$	0.058 mg/L	2.8×10^{-13}
$CuCrO_4$	Low Solubility	3.6×10^{-6}
$ZnCrO_4$	Low Solubility	NA

[3] Sillen and Martell, 1964; Brown and Lemay, 1981

Table 4.7 presents the concentrations of selected low-solubility cations and hexavalent chromium. The cations were present in the filtered bottom sample collected during the 400°C test. The concentration of hexavalent chromium was 0.288 mg/L or 2.5 X 10^{-6} mole/L. The molar concentration of CrO_4^{-2} was approximately equal to the molar sum of the cations (2.6 X10^{-6}). Therefore, it was concluded that the removal of hexavalent chromium resulted from the association and precipitation of a combination of these hexavalent chromium salts.

Table 4.7 Concentration of Selected Cations in 400°C Filtered Bottom Sample

Species	Concentration (mg/L)	Concentration (gm-mole/L)
$CrO4^{-2}$	0.288	2.5 X 10^{-6}
Ba^{+2}	0.185	7.3 X 10^{-7}
Zn^{+2}	0.111	7.6 X 10^{-7}
Cu^{+2}	0.081	4.5 X 10^{-7}
Pb^{+2}	0.225	7.0 X 10^{-7}
Σ Cations		2.6 X 10^{-6}

In contrast to the removal of soluble trivalent chromium by co-precipitation with insoluble and associated soluble salts, hexavalent chromium was removed from the liquid effluent by precipitation. This precipitation occurred when the solubility product of these low-solubility hexavalent chromium salts exceeded the Ksp value of these salts at the test conditions.

Hexavalent chromium in the 300°C test effluent represents only 13% of the total estimated chromium corrosion products. This indicates that the electrode potential and pH at the metal surface - bulk fluid boundary layer along the length of the near-isothermal reaction zone favored the generation of trivalent chromium.

The retention of hexavalent chromium in the reactor bottom at 400°C made it difficult to determine the percentage of chromium corrosion products that were the hexavalent species. However, based upon the Pourbaix diagram for chromium at critical conditions (Figure 2.8), it was possible to predict the

chromium corrosion products generated at 400°C. The conditions in the near-isothermal reaction zone (400°C and 25.0 MPa) are similar to critical condition (374°C and 21.7 MPa). An initial analysis suggested that the only chromium corrosion product in the effluent under basic pH conditions would be hexavalent chromium. However, this contradicted the experimental results. In the 400°C test, the effluent contained 0.23 mg/L of soluble trivalent chromium, which was assumed to be a corrosion product. This contradiction was resolved by assuming that the pH value of the anode region at the corroding metal surface could have ranged from 3 to 5 pH units lower than the pH value of the effluent. Inspection of the Pourbaix diagram at this adjusted range of pH values indicated that trivalent chromium was also a predicted chromium corrosion product. The lower pH values at the anode resulted from the hydrolysis reactions of Cr^{+3} and Cr^{+6} occurring at the metal surface - bulk fluid interface. These reactions are shown in Eqs. 2.15 and 2.18.

4.3 Industrial Sludge Results

The industrial sludge contained clays, a variety of paper fibers, and organic solids. This sludge was treated at two supercritical temperatures (450°C and 400°C) and one near-critical temperature (367°C). Multiple flow rates were utilized for each temperature. The concentration of total solids in the influent sludges was approximately 0.5%. Total solids were equally divided between fixed and volatile solids. The chromium concentration of the influent feed was 0.02 mg/L. Nonsoluble chromium was the only chromium specie detected in these influent sludges.

4.3.1 pH

The pH of the influent sludges and treated effluent, respectively, ranged from 6.5 to 7.2 and from 5.7 to 6.5. The tendency of the effluents to become slightly more acidic was due to the generation of large amounts of acetic acid and the slower destruction rate for relatively stable low-molecular-weight organic acids. The concentration of acetic acid in the effluents ranged from 34 mg/L to 1,206 mg/L. The lowest concentrations of acetic acid were seen in the 450°C effluents and were proportional to reaction zone residence time. Longer reaction zone retention time resulted in lower acetic acid concentration in the effluent.

As opposed to the municipal sludges, the tendency of the industrial sludge effluents to become more acidic was not counteracted by production of ammonia. Lower levels of organic-nitrogen in the influent sludge resulted in reduced ammonia concentrations in the effluents (3 mg/L to 27 mg/L).

4.3.2 Volatile Solids Reductions

The COD of the influent sludge was approximately 5,000 mg/L. However, high concentrations of clay and oxidized particulates in these effluents interfered with the Hach COD colorimetric tests. Volatile solids reduction was therefore utilized as an indicator of organic materials destruction. The typical volatile solids concentration of the influent sludge was approximately 2,700 mg/L. The volatile solids reduction for supercritical conditions ranged from 80% to 95%. Volatile solids reduction was directly related to temperature and flow rate. High temperatures and lower flow rates gave higher volatile solid destruction rates, as compared with lower temperatures and higher flow rates.

4.3.3 Hexavalent Chromium

As opposed to the municipal sludge effluents, none of the industrial sludge effluents contained detectable concentrations of hexavalent chromium. This absence of hexavalent chromium corrosion product agrees with results reported by Fisher (1971). During treatment of settled sewage sludges by WAO, the hexavalent chromium concentrations were negligible if the pH value of the effluent was mildly acidic.

4.3.4 Nonsoluble Trivalent Chromium

The concentrations of nonsoluble trivalent chromium in these effluents were minimal. As indicated by the data in Table 4.8, the soluble trivalent chromium and total trivalent chromium concentrations were similar. Composite samples (2E and 3H) collected from the reactor bottom, however, contained high concentrations of nonsoluble trivalent chromium (2.35 mg/L and 2.41 mg/L, respectively). These values were more than ten times the soluble trivalent chromium concentrations of these samples.

The high concentrations of nonsoluble trivalent chromium in the reactor bottom samples resulted from the co-precipitation of Cr^{+3}, as an impurity, during the association and precipitation of insoluble $CaCO_3$ and

$Ca_3(PO_4)_2$. This assumption is based on the high concentrations (≈ 1,850 mg/L) of Ca in the solid phase of these samples. This large concentration difference, three orders of magnitude between Ca and Cr, indicates that soluble trivalent chromium was present as a co-precipitate in this insoluble salt matrix.

The clay contained in these effluents was predominately kaolinite, an additive to the paper recycling process. The zero point of charge (pHzpc) for this clay is a pH value of 4.6 (Stumm and Morgan, 1981). All effluent pH values were above this pHzpc, so a modest amount of cation adsorption to the surface of this clay would be expected. However, the adsorption of soluble cations to the surface of clays is a relatively slow process as compared with the removal of soluble cations by co-precipitation with insoluble salts. Therefore, it appeared to be logical that nonsoluble trivalent chromium species in the reactor bottoms were not adsorbed trivalent chromium.

Table 4.8 Chromium Concentration in Industrial Sludge Effluents

Sample	Test Conditions Temp/Flow Rate (°C/gm/min)	Trivalent Chromium Total (mg/L)	Trivalent Chromium Soluble (mg/L)
1A	Feed(0.5% Solids)	0.02	<0.01
1B	400/120	0.92	1.22
1C	400/90	0.60	0.45
1D	400/60	0.97	1.11
1E	Bottom Sample	Sample line clogged	
2A	Feed(0.5% Solids)	0.02	<0.01
2B	400/120	0.21	0.27
2C	400/90	0.35	0.17
2D	450/90	0.27	0.25
2E	Bottom Sample	2.35	0.22
3A	Feed(0.5% Solids)	0.02	<0.01
3B	450/120	0.36	0.38
3C	450/60	0.47	0.52
3D	400/60	0.44	0.45
3E	400/90	0.13	0.16
3F	400/120	0.14	0.13
3G	367/90	0.24	0.21
3H	Bottom Sample	2.41	0.18

4.3.5 Soluble Trivalent Chromium

As opposed to chromium in the bottom samples, chromium in the effluent was primarily soluble trivalent chromium. Therefore, it must be assumed that trivalent chromium was not adsorbed to the surfaces of the clay present in the effluents. The absence of adsorbed trivalent chromium in the effluents offers additional evidence that nonsoluble trivalent chromium in the reactor bottoms reactor was co-precipitated soluble trivalent chromium.

As opposed to the municipal sludge results, there was no elevated concentration of soluble trivalent chromium in the bottom sediments. This finding indicated that soluble trivalent chromium was not retained in the reactor bottoms by precipitation as an associated soluble salt or by co-precipitation with other associated soluble salts. The concentrations of selected species in the filtered bottom sediments for the 2E and 3H samples are presented in Tables 4.9 and 4.10.

The concentrations of CH_3COO^-, NO_3^-, Cl^-, and Ca^{+2} in the reactor bottom samples derived from industrial and municipal sludges (400°C) were comparable. The most significant differences in these samples were lower concentrations of SO_4^{-2} and soluble trivalent chromium.

The lower concentration of SO_4^{-2} in the industrial effluents resulted from a reduced level of proteinaceous materials in the influent sludge. The industrial sludge effluent typically contained an SO_4^{-2} concentration of 15 mg/L as compared with 40 mg/L for the municipal sludge effluents. This lower concentration of proteinaceous materials was also reflected in the production of lower concentrations of NH_3 in the industrial sludge effluents.

Table 4.9 Concentration of Selected Species in 2E Filtered Bottom Sample

Species	Concentration (mg/L)	Concentration (gm-mole/L)
Soluble Cr^{+3}	0.22	3.5×10^{-6}
CH_3COO^-	<50	$<8.8 \times 10^{-4}$
NO_3^-	<50	$<8.7 \times 10^{-4}$
Cl^-	120	3.4×10^{-3}
SO_4^{-2}	<50	5.2×10^{-4}
Ca^{+2}	250	6.3×10^{-3}

Table 4.10 Concentration of Selected Species in 3H Filtered Bottom Sample

Species	Concentration (mg/L)	Concentration (gm-mole/L)
Soluble Cr^{+3}	0.18	3.5×10^{-6}
CH_3COO^-	<50	$<8.8 \times 10^{-4}$
NO_3^-	<50	$<8.7 \times 10^{-4}$
Cl^-	120	3.4×10^{-3}
SO_4^{-2}	<50	5.2×10^{-4}
Ca^{+2}	239	6.3×10^{-3}

These comparably low concentrations of SO_4^{-2} were responsible for the apparent absence of precipitated, associated soluble $NaHSO_4$ and $Ca(HSO_4)_2$ salts in the reactor bottoms. It is expected that the concentrations of SO_4^{-2} were not sufficient to generate a solubility product that exceeded the Ksp values for $Ca(HSO_4)_2$ and $NaHSO_4$ at the test conditions. Conversely, a higher concentrations of SO_4^{-2} in the municipal sludge effluent resulted in the precipitation of these associated soluble salts.

The absence of this possible association and of precipitation of $Ca(HSO_4)_2$ and $NaHSO_4$ resulted in soluble trivalent chromium not being co-precipitated with associated soluble salts. Consequently, there was not a build-up of soluble trivalent in the salt matrix that ultimately solubilized at ambient conditions.

The highest concentrations of selected species in the reactor bottom samples were for Ca^{+2} and Cl^-. These elevated concentrations are believed to have resulted from the co-precipitation of Cl^- and Ca^{+2}, as impurities, during the precipitation of $CaCO_3$ and $Ca_2(PO_4)_3$. These co-precipitated soluble species returned to the liquid phase at ambient conditions.

5.0 ENGINEERING SIGNIFICANCE

This section was developed to assess the engineering significance of experimental results. Data are provided describing chromium corrosion products generated and the behavior of chromium species in SCWO effluents.

The pH of the effluent determined the oxidation state of the chromium corrosion products. At a pH of < 7, hexavalent chromium was not detected in the effluents. Thus, hexavalent chromium generation could be prevented by neutralizing the influent sludge. It is recommended that H_3PO_4 be considered for this purpose. The PO_4^{-3} forms insoluble salts with cations present in these sludges and with normally soluble Cr^{+3}. Thus, the trivalent chromium could then be removed by precipitation as $CrPO_4$ or as a possible co-precipitate with other insoluble PO_4^{-3} salts.

Hexavalent chromium was removed from municipal sludge supercritical fluids by the association and precipitation of chromate salts. This observation indicated that municipal sludges contain the necessary cation concentrations to remove hexavalent chromium to levels of < 0.004 mg/L at SCWO conditions.

Soluble trivalent chromium corrosion products were removed from supercritical fluids by co-precipitation with SO_4^{-2}, PO_4^{-3}, and CO_3^{-2} salts. Therefore, it was established that soluble trivalent chromium could be removed from SCWO effluents as an impurity using conventional salt separation technologies.

Soluble trivalent chromium was not adsorbed to particulates during these SCWO treatment regimes. Therefore, trivalent chromium corrosion products must be removed as soluble salt species and not as adsorbed species.

6.0 CONCLUSIONS AND RECOMMENDATIONS

The objectives of this research were to identify the chromium species generated during the SCWO of wastewater sludges and to determine the behavior of these species in the SCWO environment. This section presents the conclusions and recommendations.

6.1 Conclusions

1. The pH of the effluent was an important factor in determining the oxidation state of the chromium corrosion products. At pH < 7, trivalent chromium was the only chromium corrosion species generated. If the pH was > 7, both trivalent and hexavalent chromium corrosion species were generated.

2. The removal of hexavalent chromium from these effluents was temperature-dependent. At 300°C and at a concentration of 0.035 mg/L, hexavalent chromium salts were not removed from SCWO effluents. Conversely at 400°C, these salts were removed by association and precipitation of chromate salts to concentrations of < 0.004 mg/L. These chromate salts were present as minor constituents in the reactor bottom liquids.

3. Soluble trivalent chromium was removed from sub-CWO and SCWO processes as an impurity by co-precipitation with insoluble and associated soluble salts. Soluble trivalent chromium that co-precipitated with associated soluble salts was soluble under ambient conditions. Conversely, soluble trivalent chromium that co-precipitated with the insoluble salts remained in the insoluble phase under ambient conditions. Trivalent chromium was present as a minor constituent in both the settled ash and reactor bottom liquids.

4. The removal rate of soluble trivalent chromium from these effluents was dependent on the temperature and anion concentration. At 400°C, as compared with 300°C, the removal rate was larger by a factor of approximately five. Low concentrations of SO_4^{-2} in the effluent at SCWO conditions reduced the likelihood of co-precipitation of soluble trivalent chromium with associated soluble salts.

5. A substantial amount of clay was present in the industrial sludge. Soluble trivalent chromium was not adsorbed to the oxidized clay.

6.2 Recommendations

1. This research utilized a small-scale continuous-flow reactor. The flow regimes for these experiments were in the transition and low-turbulent ranges. Consequently, insoluble and associated soluble salts were permitted to settle and collect in the reactor bottoms. Commercial-scale SCWO reactors will operate at much higher Reynolds numbers and use conventional solids separation technologies. Studies are required to determine if soluble chromium species are removed effectively from commercial-scale SCWO effluents.

2. The solubility and Ksp values for soluble trivalent and hexavalent chromium salts at different SCWO conditions are not known. Determination of these values would aid in predicting the association and precipitation of trivalent and hexavalent salts.

3. The removal of trivalent and hexavalent soluble chromium species from SCWO effluent is strongly influenced by the particular co-ion and the concentration of that co-ion. Some of these co-ions form insoluble or low-solubility chromium salts at supercritical conditions. Research to determine the tradeoffs of adding such ions to sludge influent streams for the purpose of removing soluble chromium species should be considered.

4. This research utilized wastewater sludges that contained low chromium concentrations. Wastewater sludges containing high chromium concentrations should be studied.

REFERENCES

Ahmadi, A.B., "Effects of Water Quality Parameters on Corrosion of Mild Steel, Copper and Zinc," Ph.D. Dissertation, University of Florida, Gainesville, FL, 1981.

Bramlette, T.T., et al., "Destruction of DOE/DP Surrogate Wastes with Supercritical Water Oxidation Technology," Report No. SAND90-8229, Sandia National Laboratories, Livermore, CA November 1990.

Brown, T.L., and Lemay, H.E., Chemistry–The Central Science, 2nd Edition, Prentice-Hall, Englewood Cliffs, NJ, 1981.

Buelow, S.J., et al., "Advanced Techniques for Soil Remediation: Destruction of Propellant Components in Supercritical Water," Los Alamos National Laboratory, 1990.

Clesceri, L.S., et al., eds., Standard Methods for the Examination of Water and Wastewater, 17th Ed., APHA, AWWA and WPCF; Washington, D.C., 1989.

Connolly, J.F., "Solubility of Hydrocarbons in Water Near the Critical Solution Temperature," J. Chem. Eng. Data, 11(3), 13, 1966.

Dell'Orco, P.C., Personal Communication, Balcones Research Center, The University of Texas, Austin, TX, 1991.

Dell'Orco, P.C., Gloyna, E.F., and Buelow, S.J., "The Separation of Solids from Supercritical Water," Supercritical Fluid Engineering Science Fundamentals and Applications, Kiran, E., and Brennecke, J.F., eds., ACS Symposium Series 514, American Chemical Society, Washington, D.C., 1993.

Fisher, W.J., "Oxidation of Sewage with Air at Elevated Temperatures," Water Res., 5(5), 187, 1971.

Franck, E.U., "Water and Aqueous Solutions at High Temperatures and Pressures," Pure Appl. Chem., 37, 387, 1963.

Franck, E.U., "Concentrated Electrolytes Solutions at High Temperatures and Pressures," J. Sol. Chem., 2, 339, 1973.

Franck, E.U., "Water of Properties," High Temperature High Pressure Electrochemistry in Aqueous Solutions, National Association of Corrosion Engineers, 4, 109, Houston, TX, 1976.

Gallanger, J.S., and Haar, L., "Thermophysical Properties of Water (Steam)," National Institute of Standards and Technology Standard Reference Database 10, Washington, D.C., 1985.

Habashi, F., "Kinetics of Corrosion of Metals," J. of Chem. Edu., 42(6), 318, 1965.

Helling, R.K., and Tester, J.W., "Oxidation of Simple Compounds and Mixtures in Supercritical Water: Carbon Monoxide, Ammonia and Ethanol," Environ. Sci. and Technol., 22(11), 1319, 1988.

Hong, G.T., "Supercritical Water Oxidation: Treatment of Human Waste and System Configurations Tradeoff Study," SAE Technical Paper No. 871444, Presented at the 17th Intersociety Conference of Environmental Systems, Seattle, WA, July 1987.

Huang, S., et al., "Thermodynamic Analysis of Corrosion of Iron Alloys in Supercritical Water," Supercritical Fluid Science and Technology, Johnston, K.P., and Penninger, J.M.L., eds., ACS Symposium Series 406, American Chemical Society, Washington, D.C., 1989a.

Huang, S., et al., "Electrochemical Measurements of Corrosion of Iron Alloys in Supercritical Water," Supercritical Fluid Science and Technology, Johnston, K.P., and Penninger, J.M.L., eds., ACS Symposium Series 406, American Chemical Society, Washington, D.C., 1989b.

Imai, A., "The Behavior of Chromium in the Activated Sludge Process," Ph.D Dissertation, The University of Texas, Austin, TX, 1988.

Josephson, J., "Supercritical Fluids," Environ. Sci. Technol., 16(10), 584A, 1982.

Lee, D.S., "Supercritical Water Oxidation--A Microreactor System," presented at Water Pollution Control Federation Specialty Conference, New Orleans, LA, April 1989.

Marshall, W.L., "Conductance and Equilibria of Aqueous Electrolytes over Extreme Ranges of Temperature and Pressure," Rev. Pure and Appl. Chem., 18, 167, 1968.

Marshall, W.L., "Water and Its Solution at High Temperatures and Pressures," Chemistry, 48(2), 6, 1975.

Marshall, W.L., "Predicting Conductance and Equilibrium Behavior of Aqueous Electrolytes at High Temperatures and Pressures," High Temperature High Pressure Electrochemistry in Aqueous Solutions, National Association of Corrosion Engineers, 4, 117, Houston, TX, 1976.

Martynova, O.I., "Solubility of Inorganic Compounds in Subcritical and Supercritical Water," High Temperature High Pressure Electrochemistry in Aqueous Solutions, National Association of Corrosion Engineers, 4, 131, Houston, TX, 1976.

Matthews, C.F., "Corrosion Behavior of Three High-Grade Alloys in Supercritical Water Oxidation Environments," Master's Thesis, The University of Texas, Austin, TX, 1991.

Metcalf and Eddy, Inc., "Wastewater Engineering Treatment, Disposal, and Reuse"; 3rd edition, Revised by George Tchobanoglous and Franklin L. Burton, Mc-Graw-Hill, New York, NY, 1991.

Modell, M., "Supercritical Water Oxidation," Standard Handbook for Hazardous Waste Treatment and Disposal, Freeman, H. M., ed., McGraw-Hill, New York, NY, 1986, chaps. 6-11.

Modell, M., et al., "Supercritical Water--Testing Reveals New Process Holds Promise," Solid. Waste Management, 80 August, 1982.

Muzyczko, T.M., "Symposium on Interfacial Phenomena in Corrosion Protection: A Review of Electrochemical Corrosion Fundamentals," Ind. Eng. Chem. Prod. Res. Dev., 17(2), 169, 1978.

Peron, D.L., The Electrochemistry of Corrosion, National Association of Corrosion Engineers, Houston, TX, 1991.

Pisigan, R.A., "The Development of New Equations for the pH of Calcium Carbonate Saturation and Corrosion In Water Systems," Ph.D. Dissertation, University of Florida, Gainesville, FL, 1981.

Pourbaix, M., Atlas of Electrochemical Equilibria in Aqueous Systems, Pergamon Press, New York, NY, 1976.

Pray, H.A., Schweickert, B.H., and Minnich, B.H., "Solubility of Hydrogen, Oxygen, Nitrogen, and Helium in Water at Elevated Temperature," Ind. Eng. Chem., 44, 1146, 1952.

Shanableh, A., "Subcritical and Supercritical Water Oxidation of Industrial, Excess Activated Sludge," Ph.D. Dissertation, The University of Texas, Austin, TX, 1990.

Sillen, L.G., and Martell, A.E., Stability Constants of Metal Ion Complexes, Special Publication No. 17, The Chemical Society, London, England, 1964.

Steigerwald, R.F., "Electrochemistry of Corrosion," Corrosion, 24, 10, 1968.

Stumm, W., and Morgan, J.J., Aquatic Chemistry, 2nd edition, John Wiley and Sons, New York, NY, 1981.

Sychev et al., Thermodynamic Properties of Oxygen, Hemisphere Publishing Corp., New York, NY, 1987.

Takashashi, Y., et al., "Subcritical and Supercritical Water Oxidation of CELESS Model Waste," in Controlled Ecological Life Support Systems: Natural and Artificial Ecosystems, NASA Conference Publication 10040, XXVII COSPAN meeting at Espoo, Finland, July 1989.

Thomas, A.J., "Corrosion Behavior of High-Grade Alloys in the Supercritical Water Oxidation of Sludges," Master's Thesis, The University of Texas, Austin, TX, 1990.

Thomason, T.B., and Modell, M., "Supercritical Water Destruction of Aqueous Wastes," Hazard. Waste, 1(4), 453, 1984.

Todheide, K., "Water at High Temperatures and Pressures," Water: A Comprehensive Treatise, Franks, F., ed., Plenum Press, New York, NY, 1972.

Todheide, K., and Franck, E.U., "Das Zweiphasehgeiet und Kritische Kurve in System Kohlendioxid-Wasser bis zu Drucken von 3500 bar," Z. Phys. Chem., 37, 387, Frankfurt, Germany, 1963.

Tongdhamachart, C., "Supercritical Water Oxidation of Anaerobically Digested Municipal Sludge," Ph.D. Dissertation, The University of Texas, Austin, TX, 1990.

Uematsu, M. and Franck, E.U., "Static Dielectric Constant of Water and Steam," J. Phy. Chem. Ref. Data, 9(4), 1921, 1980.

Uhling, R.H., Corrosion and Corrosion Control, John Wiley and Sons, New York, NY, 1971.

Weast, R.C., Editor-in-Chief, Handbook of Chemistry and Physics, CRC Press, Inc., Boca Raton, FL, 1985.

Wilmanns, E.C., "Supercritical Water Oxidation of Volatile Acids," Master's Thesis, The University of Texas, Austin, TX, 1990.

Wilmanns, E.C., Unpublished Treatability Study, Balcones Research Center, The University of Texas, Austin, TX, 1992.